



HAL
open science

New pyrido[3,4-g]quinazoline derivatives as CLK1 and DYRK1A inhibitors: synthesis, biological evaluation and binding mode analysis

Helmi Tazarki, Wael Zeinyeh, Yannick J. Esvan, Stefan Knapp, Deep Chatterjee, Martin Schröder, Andreas C. Joerger, Jameleddine Khiari, Béatrice Josselin, Blandine Baratte, et al.

► To cite this version:

Helmi Tazarki, Wael Zeinyeh, Yannick J. Esvan, Stefan Knapp, Deep Chatterjee, et al.. New pyrido[3,4-g]quinazoline derivatives as CLK1 and DYRK1A inhibitors: synthesis, biological evaluation and binding mode analysis. *European Journal of Medicinal Chemistry*, 2019, 166, pp.304-317. 10.1016/j.ejmech.2019.01.052 . hal-02150788

HAL Id: hal-02150788

<https://hal.science/hal-02150788v1>

Submitted on 21 Oct 2021

HAL is a multi-disciplinary open access archive for the deposit and dissemination of scientific research documents, whether they are published or not. The documents may come from teaching and research institutions in France or abroad, or from public or private research centers.

L'archive ouverte pluridisciplinaire **HAL**, est destinée au dépôt et à la diffusion de documents scientifiques de niveau recherche, publiés ou non, émanant des établissements d'enseignement et de recherche français ou étrangers, des laboratoires publics ou privés.



Distributed under a Creative Commons Attribution - NonCommercial 4.0 International License

New pyrido[3,4-g]quinazoline derivatives as CLK1 and DYRK1A inhibitors: synthesis, biological evaluation and binding mode analysis

Helmi Tazarki^{‡,§}, Wael Zeinyeh[‡], Yannick J. Esvan[‡], Stefan Knapp^{l,#}, Deep Chatterjee^{l,#}, Martin Schröder^{l,#}, Andreas C. Joerger^{l,#}, Jameleddine Khiari[§], Béatrice Josselin[†], Blandine Baratte[†], Stéphane Bach[†], Sandrine Ruchaud[†], Fabrice Anizon[‡], Francis Giraud^{‡,*}, Pascale Moreau^{‡,*}

[‡] Université Clermont Auvergne, CNRS, SIGMA Clermont, ICCF, F-63000 Clermont-Ferrand, France.

[§] Carthage University, Laboratory of Organic and Analytical Chemistry (ISEFC), Tunis, Tunisia.

^l Institute of Pharmaceutical Chemistry, Johann Wolfgang Goethe University, Max-von-Laue-Str. 9, 60438, Frankfurt am Main, Germany.

[#] Buchmann Institute for Molecular Life Sciences and Structural Genomics Consortium (SGC), Max-von-Laue-Str. 15, 60438, Frankfurt am Main, Germany.

[†] Sorbonne Université, CNRS, Plateforme de Criblage KISSf (Kinase Inhibitor Specialized Screening Facility), Protein Phosphorylation and Human Diseases Unit, Station Biologique, Place Georges Teissier, F-29688 Roscoff, France.

* Corresponding authors

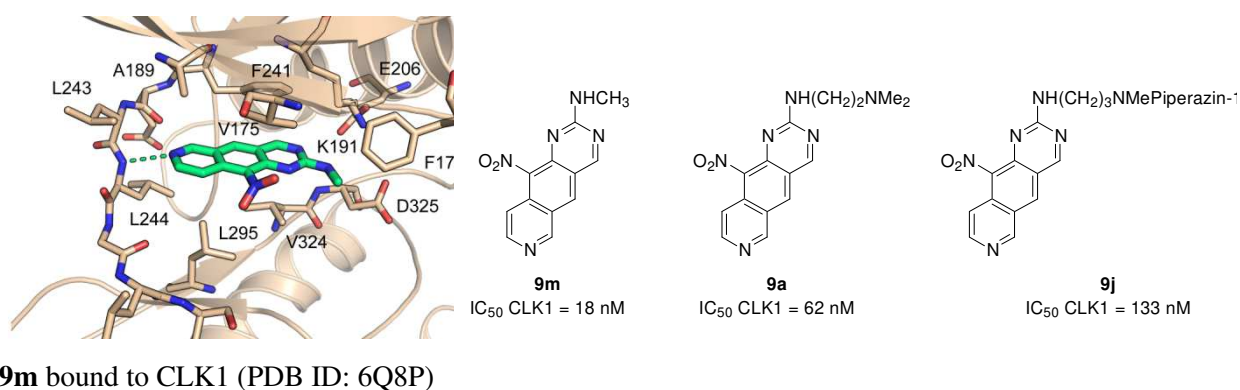
(PM) Tel: +33 (0) 4 73 40 79 63. E-mail: pascale.moreau@uca.fr

(FG) Tel: +33 (0) 4 73 40 71 27. E-mail: francis.giraud@uca.fr

Abstract

Cdc2-like kinase 1 (CLK1) and dual specificity tyrosine phosphorylation-regulated kinase 1A (DYRK1A) are involved in the regulation of alternative pre-mRNA splicing. Dysregulation of this process has been linked to cancer progression and neurodegenerative diseases, making CLK1 and DYRK1A important therapeutic targets. Here we describe the synthesis of new pyrido[3,4-g]quinazoline derivatives and the evaluation of the inhibitory potencies of these compounds toward CDK5, CK1, GSK3, CLK1 and DYRK1A. Introduction of aminoalkylamino groups at the 2-position resulted in several compounds with low nanomolar affinity and selective inhibition of CLK1 and/or DYRK1A. Their evaluation on several immortalized or cancerous cell lines showed varying degree of cell viability reduction. Co-crystal structures of CLK1 with two of the most potent compounds revealed two alternative binding modes of the pyrido[3,4-g]quinazoline scaffold that can be exploited for future inhibitor design.

Graphical abstract



Introduction

Protein kinases are important cellular targets for the development of novel chemical probes and drugs in many therapeutic areas, including cancer, neurodegenerative disorders, inflammation or pain therapy. To date, more than five hundred protein kinases have been identified in the human kinome. All of them share the same co-factor (ATP), and the ATP binding pocket shows high structural conservation in most of them. Developing kinase inhibitors that display selectivity within the human kinome, therefore, remains a major challenge [1]. However, as shown by FDA approved drugs, especially in oncology, absolute selectivity for a single kinase is not always needed [2]. As part of our ongoing efforts toward the development of potent and selective kinase inhibitors, we recently described pyrido[3,4-g]quinazolines as inhibitors of Cdc2-like kinases (CLK1) and dual specificity tyrosine phosphorylation-regulated kinases (DYRK1A) [3]. CLK1 and DYRK1A are involved in the regulation of alternative pre-mRNA splicing via SR-protein phosphorylation, and dysfunction of this tightly regulated process is linked to the progression of cancer, neurodegenerative diseases, and viral infections [4,5]. As reported in recent reviews, various chemical scaffolds could lead to potent DYRK1A and/or CLK1 inhibitors [6-9]. We carried out a structure-activity relationship (SAR) study around the tricyclic pyridoquinazoline scaffold. Previous results demonstrated that the substitution by nitro/amino groups at the 10-position is essential to target CLK1 and/or DYRK1A kinases [3]. The introduction of alkyl/aryl substituents at the 5-position led to a change in the kinase inhibition profile, as 5-substituted derivatives exhibited improved potencies toward CDK5/GSK3, while CLK1/DYRK1A inhibition was impaired (Figure 1A) [10]. Since modification of this heteroaromatic scaffold resulted in a major change in activity and selectivity, we decided to further extend the SAR studies on the pyrido[3,4-g]quinazoline scaffold by varying the substitution at the 2-position (Figure 1A).

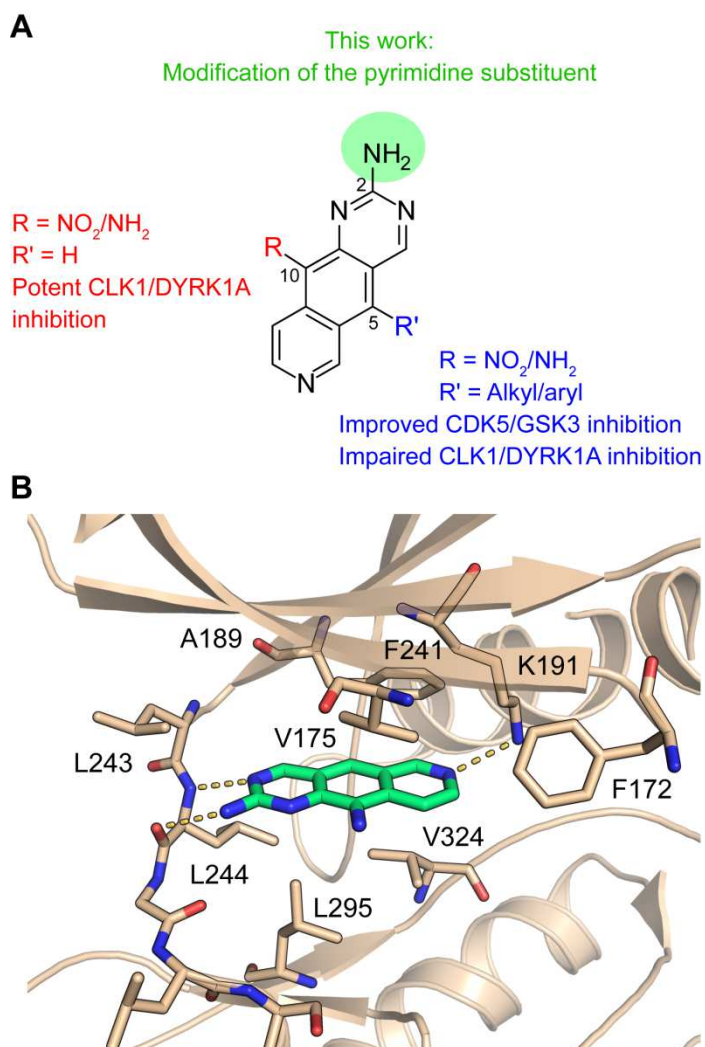


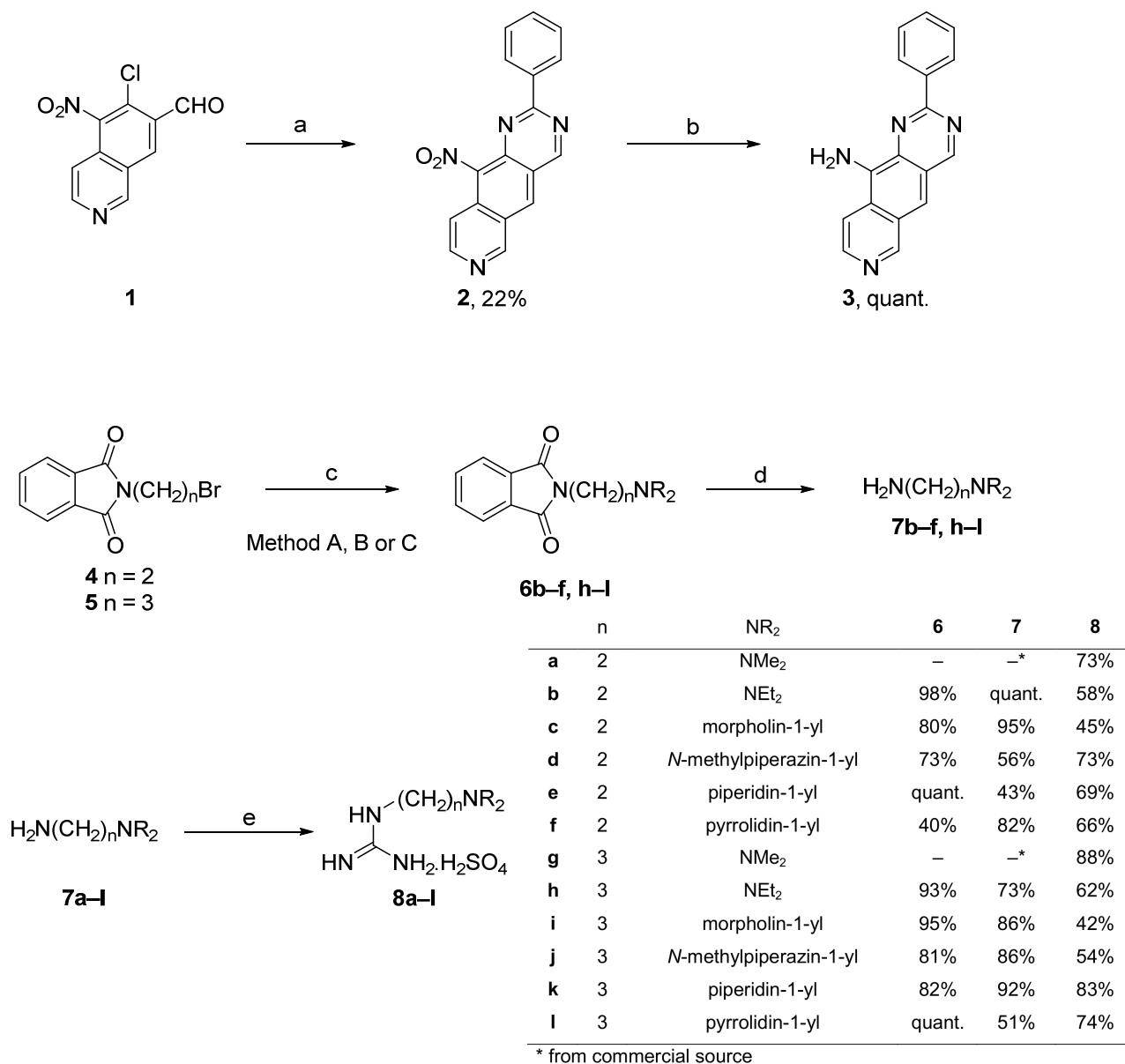
Figure 1. Design strategy for the optimization of pyrido[3,4-g]quinazoline-based kinase inhibitors. A) Structures of pyrido[3,4-g]quinazolines identified as CLK1/DYRK1A protein kinase inhibitors, highlighting earlier SAR results (blue and red) [3,10] and the optimization strategy employed in this work. B) Structure of the lead compound ($R = \text{NH}_2$, $R' = \text{H}$) bound to the ATP binding site of CLK1 (PDB ID: 5J1V). Hydrogen bonds between the compound and CLK1 are shown as dashed lines.

Results and discussion

Synthesis of compound library

Analysis of the binding mode of the best CLK1/DYRK1A inhibitor of the pyrido[3,4-g]quinazolines series showed that the aminopyrimidine moiety forms two hydrogen-bonds with the backbone amine and carbonyl group of Leu244 upon binding to CLK1 (Figure 1B). Additionally, the pyridine nitrogen atom is hydrogen-bonded to the Lys191 side chain [3]. Our aim was to extend

this lead compound by adding a series of aminoalkylamino groups at the 2-position to figure out if this alters the potency or selectivity of the compounds. To confirm the importance of the amino group at the pyrimidine moiety 2-position in the interaction with the targeted kinases, we first synthesized presumed inactive analogues **2** and **3** missing the 2-amino function, using benzamidine hydrochloride salt. Compound **2** was obtained in 22% yield by reacting isoquinoline **1**, which was prepared according to a previously reported procedure [3], with benzamidine hydrochloride salt. The reduction of the nitro group by catalytic hydrogenation led quantitatively to **3** (Scheme 1).

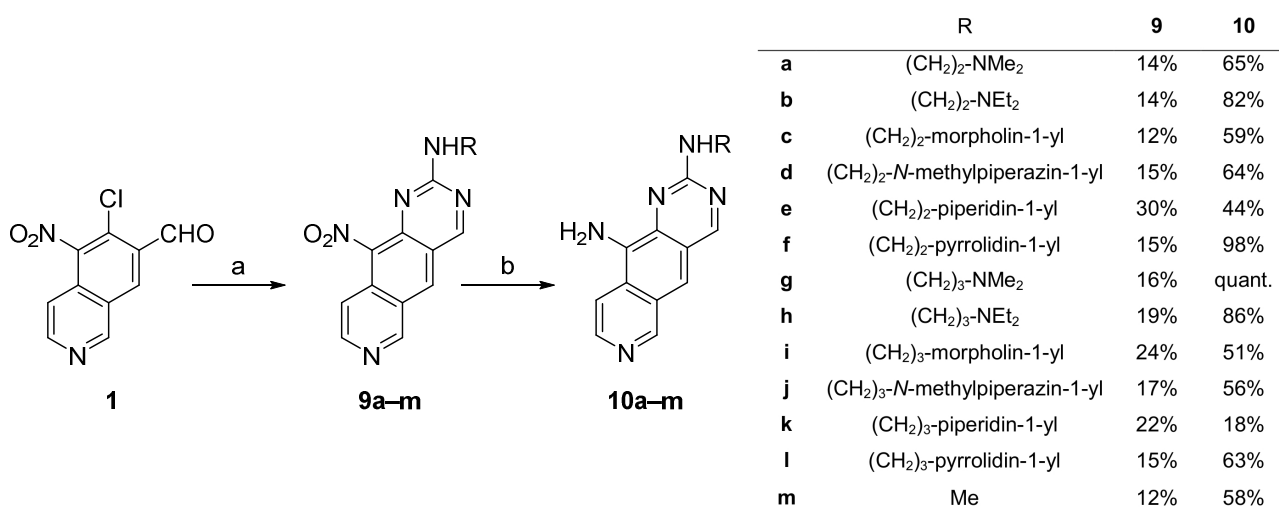


Scheme 1. Synthesis of compounds **2**, **3** and diversely substituted guanidines **8a-l**. Reagents and conditions: (a) Benzamidine HCl, DMA (b) H₂, Pd/C, CH₂Cl₂/MeOH 1:1 (c) Method A: **4** or **5**,

DIPEA, amine, DMF; Method B: **4** or **5**, K₂CO₃, amine, CH₃CN; Method C: **4** or **5**, amine, toluene (d) H₂NNH₂.H₂O, EtOH (e) *O*-methylisourea bisulfate salt, H₂O.

We then condensed **1** with diversely substituted guanidines in order to modify the substituent at position 2. The preparation of guanidines that were not commercially available started from phthalimides **4** or **5**, which were reacted with various amines to give **6b-f**, **h-l** in 40% to quantitative yields (Scheme 1). This step was performed according to published procedures (method A [11], method B [12], and method C [13]). After hydrazinolysis, amines **7b-f**, **h-l** were obtained in acceptable yields (43% to quantitative). Reaction of commercially available (**7a**, **7g**) or prepared amines (**7b-f**, **h-l**) with *O*-methylisourea bisulfate [14] led to the desired guanidines **8a-l** in acceptable to good yields (42% to 88%).

Next, different *N*-substituted-aminopyrimidines **9a-m** were obtained by reaction between isoquinoline **1** and the guanidine bisulfates. Reactions were performed using K₂CO₃ as a base in DMA [15] under conventional heating conditions. Finally, the nitro derivatives were reduced to their amino analogues **10a-m** under hydrogen atmosphere to further extend the compound library (Scheme 2).



Scheme 2. Synthesis of compounds **9a-m** and **10a-m**. Reagents and conditions: (a) Guanidine hemisulfate **8a-m** (**8m** commercially available as chlorhydrate salt), K₂CO₃, DMA (b) H₂, Pd/C, CH₂Cl₂ or CH₂Cl₂/MeOH (8:2).

Kinase inhibition assays

The inhibitory potency toward CDK5/p25, CLK1, DYRK1A, CK1 δ/ϵ and GSK-3 α/β of nitro derivatives **2**, **9a-m**, amino analogues **3**, **10a-m**, references **9** (R = H) and **10** (R = H) was evaluated (Table 1).

Table 1. Kinase inhibition assays (% residual kinase activity).

Cpds	Kinase inhibition (% residual activity and IC ₅₀ values) ¹									
	CDK5		CLK1		DYRK1A		CK1		GSK3	
	10 μ M	1 μ M	10 μ M	1 μ M	10 μ M	1 μ M	10 μ M	1 μ M	10 μ M	1 μ M
2	62	100	17	71	38	100	57	100	100	100
3	65	92	32	68	41	80	51	62	40	85
Ref 9 (R=H)	> 10 ⁴ nM		(69 nM)		(620 nM)		(780 nM)		(2.2 10 ³ nM)	
9a	52	100	5	22	17	89	36	100	21	70
			(62 nM)							
9b	79	100	8	46	47	88	78	91	26	74
9c	69	100	5	36	20	73	75	93	43	88
9d	77	84	0	32	6	32	38	63	22	69
9e	85	96	1	42	26	52	37	81	1	39
9f	83	100	7	27	29	83	73	92	33	81
9g	64	100	3	27	31	84	59	86	24	80
9h	50	100	4	31	23	72	59	87	24	92
9i	60	100	3	14	10	68	38	100	15	76
			(120 nM)							
9j	48	100	8	22	3	54	32	92	2	59
			(133 nM)							
9k	53	100	7	16	6	56	34	100	24	76
			(125 nM)							
9l	50	100	5	37	6	87	37	100	24	78
9m	38	73	2	5	13	39	45	98	51	70
			(18 nM)							
Ref 10 (R = H)	(4.8 10 ³ nM)		(41 nM)		(28 nM)		(5.8 10 ³ nM)		(9.1 10 ³ nM)	
10a	86	96	21	51	32	60	82	78	48	58
10b	40	97	3	31	6	49	60	91	34	73
10c	10	52	4	27	1	17	34	77	24	76
					(197 nM)*					
10d	55	88	4	21	2	19	70	100	22	44
			(210 nM)		(120 nM)					
10e	76	95	11	44	16	37	52	74	24	43

10f	51	100	4	33	7	54	61	90	29	62
10g	34	77	1	14	1	17	61	96	10	36
			(120 nM)		(120 nM)					
10h	20	68	2	21	2	24	45	68	22	61
			(160 nM)		(80 nM)					
10i	23	67	4	20	6	5	24	53	6	41
			(290 nM)		(23 nM)					
10j	15	49	6	8	1	4	30	61	4	35
			(117 nM)		(20 nM)					
10k	62	100	4	30	4	26	48	76	30	51
10l	44	86	4	26	1	25	23	69	23	50
					(90 nM)					
10m	3	33	1	9	1	27	60	85	40	79
			(274 nM)*							

¹IC₅₀ values were determined when the residual kinase activity was $\leq 25\%$ at a compound concentration of 1 μM (given in parentheses). IC₅₀ values for references **9** and **10** (R = H) as previously reported [3]. Kinase activities were assayed in triplicate in the presence of 15 μM ATP. Typically, the standard deviation of single data points was below 10%. All assays were performed using a ³²P radioassay in the presence of 15 μM ATP (method A), except for the determination of the two IC₅₀ values marked with an asterisk that was carried out using the ADP-Glo assay in the presence of 10 μM ATP (method B).

CLK1 and DYRK1A were generally the most strongly inhibited kinases (Table 1). A similar inhibition profile was already observed for the lead compound of this series [3]. As expected, compounds **2** and **3**, lacking the amino group at the 2-position of the pyrimidine moiety, did not exhibit any significant inhibitory effect toward the kinases tested. These results are in accordance with the binding mode of the lead compound for this series in the co-crystal structure with CLK1 (Figure 1B), showing that the amino group forms a hydrogen bond with Leu244 in the hinge region. All N-2 substituted compounds of the nitro (**9a-9m**) or amino (**10a-10m**) series were active toward CLK1 with residual kinase activities $\leq 50\%$ when tested at 1 μM , indicating that the aminoalkylamino groups at the 2-position did not cause major steric hindrance within the CLK1 pocket. DYRK1A inhibition, however, was generally less effective, in particular for the nitro series, with only 5 derivatives (**9d**, **9e**, **9j**, **9k**, **9m**) leading to residual kinase activities around or $< 50\%$ when tested at 1 μM . Thus, several nitro derivatives, particularly **9a**, **9i-9k**, and **9m**, exhibited a better activity toward CLK1. The best selectivity profiles for CLK1 over DYRK1A were found for **9a** bearing a dimethylaminoethyl group and **9m** bearing a methyl group, with IC₅₀ values against CLK1 of 62 nM and 18 nM, respectively.

Amino derivatives **10a-10m** displayed inhibitory potencies toward both CLK1 and DYRK1A in the micro/submicromolar range, with the notable exception of compounds **10i** and **10j**. Those two compounds with either a 3-(morpholin-1-yl)propyl group (**10i**) or a 3-(*N*-methylpiperazin-1-yl)propyl group (**10j**) were particularly active toward DYRK1A, with IC₅₀ values of 23 nM and 20 nM, respectively, and a more than 5-fold selectivity for DYRK1A over CLK1 (12.6 for **10i**, 5.9 for **10j**). In comparison, amino analogue reference (**10**, R = H, Scheme 2) exhibited lower selectivity with only 1.5 times better activity toward DYRK1A [3]. These results demonstrated an improvement of selectivity in the amino series.

Biological evaluation in cancer cells

As CLK1 and DYRK1A upregulation plays a key role in various cancer types, the compounds exhibiting the best kinase inhibitory potencies (**9a**, **9i**, **9j**, **9m**, **10d**, **10g**, **10i**, **10j**, **10l**) were evaluated in hTERT-immortalized retinal pigment epithelial (RPE1) cells and four cancer cell lines, HCT116 (colon carcinoma), MDA-MB231 (breast adenocarcinoma), SH-SY5Y (neuroblastoma), and U-2 OS (bone osteosarcoma). Cellular activities are given as % cell viability at a compound concentration of 2 μM compared with control DMSO treated cells (Table 2). Staurosporine was used as a positive control. Treatment with many compounds resulted in less than 25% of viable cells after 48 h in comparison to DMSO treated cells, both with the non-tumor and tumor cell lines. Indeed, all compounds were active toward the cell lines tested and induced viability reductions of more than 50%, except compounds **9i**, **9m** and **10d** on SH-SY5Y cells and for **10l** on hTERT-RPE1 and SH-SY5Y cells. The reference compound (**10**, R = H, Scheme 2) as well as three new 10-amino derivatives, **10g**, **10i** and **10j**, were particularly active toward all five cell lines, including hTERT-RPE1, with only 0% to 15% of remaining cellular viability. This lack of selectivity suggests that these amino analogues are too toxic to be considered as potential drug candidates.

Table 2. Effects of pyrido[3,4-*g*]quinazoline-based kinase inhibitors on the viability of cancer and non-cancer cells.

	hTERT-RPE1	HCT116	MDA-MB231	SH-SY5Y	U-2 OS
Compound	Viability ¹ (%)	Viability (%)	Viability (%)	Viability (%)	Viability (%)
Ref 10 (R = H)	0.2 ± 0.4	1.3 ± 0.0	43.4 ± 0.4	0.9 ± 0.3	0.4 ± 0.1
9a	29.2 ± 0.7	13.3 ± 0.8	9.4 ± 0.6	42.7 ± 0.4	3.3 ± 0.8
9i	31 ± 3	16.8 ± 0.7	39 ± 1	54 ± 2	27 ± 1
9j	25.8 ± 0.3	9.7 ± 0.5	11.7 ± 0.9	36 ± 2	2.5 ± 0.7

9m	36 ± 1	22 ± 1	41.0 ± 0.6	52 ± 2	19.5 ± 0.6
10d	19.4 ± 0.1	6.1 ± 0.9	21.7 ± 0.4	62 ± 3	13 ± 1
10g	0 ± 0	0 ± 0	0.4 ± 0.1	0.0 ± 0.0	0 ± 0
10i	0.0 ± 0.1	0.8 ± 0.1	15 ± 1	3.6 ± 0.9	6.4 ± 0.9
10j	0 ± 0	0 ± 0	3.6 ± 0.8	0.1 ± 0.1	0.1 ± 0.1
10l	52 ± 2	21 ± 6	22 ± 1	92.2 ± 0.3	33 ± 2
Staurosporine	9.1 ± 0.8	27 ± 2	3.9 ± 0.5	9.4 ± 0.1	0.4 ± 0.4

¹Cellular viability (%) at a compound concentration of 2 μM after 48 hours compared with untreated cells. Cell viability was assayed in triplicate, and mean value ± SD are given.

Most interesting compounds, **9a** and **9j**, were slightly more potent in killing U-2 OS cancer cells than hTERT-RPE1 cells, showing that, compared to **10** (R = H), selectivity could be enhanced by introducing alkyl or aminoalkyl groups on the amine group at the 2-position of the pyrido[3,4-g]quinazoline scaffold. However, a more detailed study of this series cellular effect would be of valuable interest to evaluate its potential, as well as additional structural modifications to further enhance the selectivity of this compound class for cancer cells.

Structural analysis of the binding mode of compounds **9m** and **10i** in complex with CLK1

To provide insights into the binding modes of our 2-amino-substituted pyrido[3,4-g]quinazolines, we determined the crystal structures of **9m** and **10i** in complex with CLK1 at 3.0 and 2.3 Å resolution, respectively. Interestingly, for compound **10i** bearing an amino group at the 10-position and a morpholinopropylamino substituent at the 2-position, we observed two overlapping alternative binding modes of this highly symmetrical molecule where the central ring system is tightly packed between a series of hydrophobic side chains, including Val175, Phe241, Leu295, and Val324 (Figure 2A/B). In both orientations, a nitrogen atom of the pyrido[3,4-g]quinazoline scaffold forms a hydrogen bond with the backbone nitrogen of Leu244 in the hinge region, and a nitrogen in the distal ring forms a water-mediated hydrogen bond with the Glu206 side chain in the back pocket. Details of this interaction network in the back pocket with corresponding distances are shown in Figure 2C. The secondary amino group introduced at C-2 of the tricycle interacts with either the backbone oxygen of Leu244 (as seen for the lead compound) or points in the direction of the Lys191-Glu206 salt bridge, but without forming additional electrostatic interactions with the latter. There was no clear electron density to unambiguously model the morpholino group in both cases, indicating that it is very flexible and does not interact with CLK1 in a defined orientation. This may explain why this compound is less potent against CLK1 than against DYRK1A.

The CLK1-**9m** complex was solved in a different crystal form with three molecules in the asymmetric unit. There was a preferred binding mode of the inhibitor, with the 2-aminomethyl substituent facing the Lys191-Glu206 salt bridge and packing against the aromatic ring of Phe172 (Figure 2D). In this orientation, the pyridine nitrogen forms a hydrogen bond with the Leu244 backbone nitrogen in the hinge region (3.0 Å distance). The presence of a minor second conformation, however, cannot be ruled out. The distance between the Lys191 side chain amine and the exocyclic nitrogen of **9m** is 3.2-3.6 Å, and the distance to the proximal ring nitrogen of the pyrimidine is 3.7-3.9 Å, just outside the range for hydrogen bonding. It is likely that the compound also forms a water-mediated hydrogen bond with Glu206 and the backbone nitrogen of Asp325 (as seen in the CLK1 complex with **10i**), which could not be unambiguously modelled due to the low resolution of the data set. Overall, this arrangement enables favorable electrostatic interactions in the back pocket and might be further stabilized via the adjacent side chain carboxylate of Asp325, which is within 4 Å distance of the exocyclic nitrogen. To assess the contribution of the different side chains or structural waters to stabilizing this binding mode in more detail, a high-resolution structure would be needed.

Interestingly, the lead compound that formed the starting point for this SAR study adopts a flipped orientation where the 2-amino group forms a hydrogen bond with the backbone oxygen of Leu244, and the pyridine nitrogen interacts with the Lys191 side chain (Figure 1B) [3]. Taken together, comparison of the new CLK1-inhibitor complexes with the binding mode of the parent molecule indicates that the pyrido[3,4-*g*]quinazoline scaffold can bind in two alternative orientations, depending on the nature of the ring substituents, which can be exploited for the design of inhibitors with improved potency and selectivity.

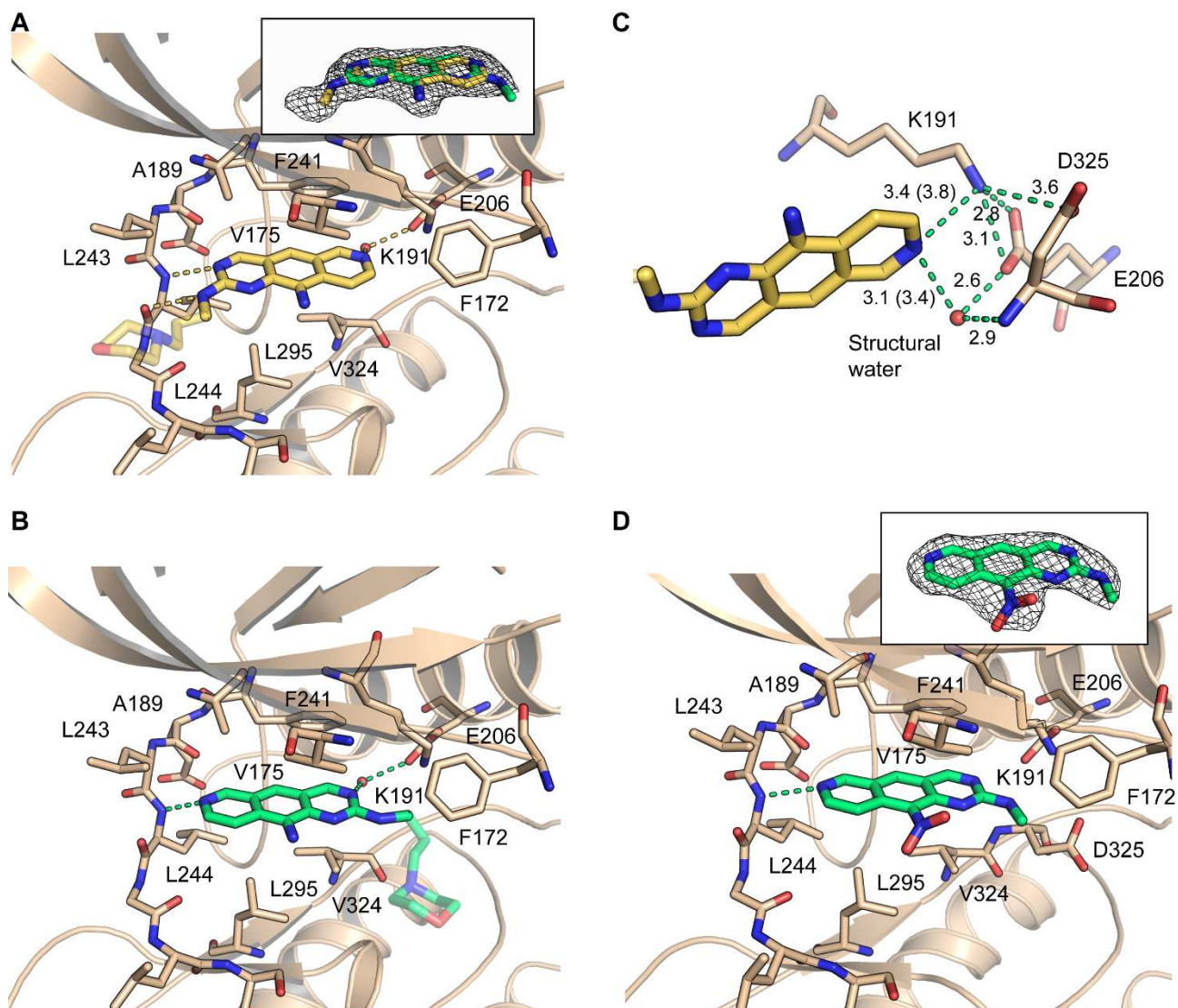


Figure 2. Structures of 2-substituted pyrido[3,4-g]quinazolines bound to CLK1. (A-B) Crystal structure of the CLK1-**10i** complex. Compound **10i** bound in two alternative orientations shown as yellow (A) and green (B) stick models, respectively. Parts of the inhibitor that were not clearly resolved in the crystal structure are shown as transparent sticks. The inset shows a $2F_o-F_c$ electron density map for the modeled inhibitor at a contour level of 1.0σ . Hydrogen bonds between the inhibitor and the CLK1 hinge region and a water-mediated contact with Glu206 are highlighted with dashed lines. (C) Close-up view of the water-mediated hydrogen bond in the back-pocket region of the CLK1-**10i** complex. Relevant distances for electrostatic interactions are highlighted as green dashed lines, and the corresponding values are given in Å. For clarity, only one conformer is shown. Distances to the pyrimidine ring nitrogen of the second conformer are given in parentheses. (D) Crystal structure of the CLK1-**9m** complex (chain B). The inset shows a $2F_o-F_c$ electron density map for the modeled inhibitor at a contour level of 1.4σ . The hydrogen bond of the inhibitor with

the hinge region is highlighted as a green dashed line. To confirm a potential water-mediated hydrogen bond of one of the pyrimidine nitrogens, as observed in the CLK1-**10i** complex, a higher resolution than the 3.0 Å of the current structure would be needed.

Conclusion

A new series of pyrido[3,4-*g*]quinazolines with diverse substitutions at the 2-position and either an amino or a nitro group at the 10-position was synthesized and evaluated against five protein kinases (CDK5/p25, CLK1, DYRK1A, CK1 δ/ϵ , and GSK-3 α/β). The results demonstrated that the aminopyrimidine part is essential to the kinase inhibitory potency of this series (compounds **2** and **3**). The most strongly inhibited kinases were CLK1 and DYRK1A, with a better selectivity toward CLK1 for 10-nitro derivatives (**9a**, **9m**), whereas 10-amino derivatives were more selective toward DYRK1A (**10i**, **10j**). Evaluation of the cellular activities of the most active compounds revealed that compounds **9a** and **9j** are slightly more active toward U-2 OS cancer cells, compared with a non-cancer cell line (hTERT-RPE1). Interestingly, structural analysis of the binding modes of two of the most potent binders showed that they can adopt alternative binding modes in the ATP-binding pocket of CLK1, depending on the substitution pattern of the heteroaromatic scaffold. Taken together our data provide a framework for the development of potent and selective CLK1/DYRK1A inhibitors for potential treatment of cancers and neurodegenerative diseases.

Experimental section

4.1 Chemistry

4.1.1. General

Starting materials were obtained from commercial suppliers and used without further purification. Solvents were distilled prior to use. IR spectra were recorded on a Shimadzu FTIR-8400S spectrometer ($\bar{\nu}$ in cm^{-1}). NMR spectra, performed on a Bruker AVANCE 400 (^1H : 400 MHz, ^{13}C : 100 MHz), are reported in ppm using the solvent residual peak as an internal standard; the following abbreviations are used: singlet (s), doublet (d), triplet (t), quadruplet (q), quintet (quint), doublet of doublet (dd), multiplet (m), broad signal (br s). High resolution mass spectra (ESI+) were determined on a high-resolution Waters Micro Q-ToF apparatus (UCA-Partner, Université Clermont Auvergne, Clermont-Ferrand, France). Chromatographic purifications were performed by column chromatography using 40–63 μm silica gel. Reactions were monitored by TLC using fluorescent silica gel plates (60 F254 from Merck). Melting points were measured on a Stuart SMP3 apparatus and are uncorrected. The purity of key compounds **9a**, **9j**, **9m**, **10i** and **10j** was established to be >

95% by HPLC analysis using a Hitachi liquid chromatograph (Oven 5310, 30 °C; Pump 5160; DAD detector 5430) and a C18 Acclaim column (4.6 mm x 250 mm, 5 μm, 120 Å). Detection wavelength was 240 nm for nitro derivative/280 nm for amino analogues, and flow rate 0.5 mL/min. Gradient elution used (A) water/0.1% TFA; (B) acetonitrile: 95:5 A/B for 5 min then 95:5 A/B to 5:95 A/B in 25 min and then 5:95 A/B for 10 min.

4.1.2 10-Nitro-2-phenylpyrido[3,4-g]quinazoline (2)

A suspension of compound **1** (50 mg, 0.21 mmol) and benzamidine hydrochloride (66 mg, 0.42 mmol) in DMA (2 mL) was degassed with argon for 30 min then heated at 75 °C (oil bath) for a total time of 2 h. After completion of the reaction, EtOAc was added. The resulting slurry was filtered on a pad of Celite and washed with EtOAc. The organic layer was washed with water and brine, dried (MgSO₄) and the volatiles were removed under reduced pressure. The residue was purified twice by flash chromatography using firstly EtOAc/cyclohexane (7:3) and secondly CH₂Cl₂/AcOEt (1:1), yielding compound **2** (14 mg, 0.046 mmol, 22%) as a light brown-yellow powder. Mp > 260 °C; R_f = 0.2 (EtOAc/Cyclohexane 7:3). IR (ATR): 1627, 1594, 1565, 1525, 1425, 1381, 1293, 1271, 1148 cm⁻¹. ¹H NMR (400 MHz, DMSO-*d*₆) δ 7.60 – 7.71 (3H, m), 7.89 (1H, d, *J* = 6.3 Hz), 8.56 – 8.63 (2H, m), 8.78 (1H, d, *J* = 6.3 Hz), 9.53 (1H, s), 9.89 (1H, d, *J* = 1.1 Hz), 10.23 (1H, s); ¹³C NMR (100 MHz, DMSO-*d*₆): Not recorded due to low solubility. HRMS (ESI+) calcd for C₁₇H₁₁N₄O₂ (M+H)⁺ 303.0876, found 303.0879.

4.1.3 2-Phenylpyrido[3,4-g]quinazolin-10-amine (3)

To a solution of 11 mg (0.036 mmol) of compound **2** in 4 mL of CH₂Cl₂/MeOH 1:1 at room temperature was added 2 mg of Pd/C. The suspension was stirred under 1 atm of H₂ in the dark at room temperature overnight. After filtration over Celite in a Pasteur pipette, washing with CH₂Cl₂ and concentration, compound **3** (9.7 mg, 0.036 mmol, quant. yield) was isolated without further purification as a dark red powder. Mp: degradation; R_f = 0.25 (EtOAc/Cyclohexane 7:3). IR (ATR): 3420-2602, 1623, 1591, 1541, 1405, 1362 cm⁻¹. ¹H NMR (400 MHz, DMSO-*d*₆) δ 7.39 (2H, br s, NH₂), 7.55-7.60 (3H, m), 7.99 (1H, s), 8.28 (1H, d, *J* = 6.4 Hz), 8.38 (1H, d, *J* = 6.4 Hz), 8.78 (2H, dd, *J* = 9.6 Hz, *J* = 1.6 Hz), 9.43 (1H, s), 9.81 (1H, s); ¹³C NMR (100 MHz, DMSO-*d*₆) δ 111.1, 115.9 (CH_{arom}), 128.3 (2CH_{arom}), 128.7 (2CH_{arom}), 130.6, 139.8, 154.8, 163.4 (CH_{arom}), 114.9, 122.4, 127.5, 132.3, 137.5, 141.6, 156.1 (C_{arom}). HRMS (ESI+) calcd for C₁₇H₁₃N₄ (M+H)⁺ 273.1135, found 273.1135.

4.1.4 2-(2-*N,N*-Diethylaminoethyl)-1*H*-isoindole-1,3(2*H*)-dione (**6b**): prepared according to method C [13] in 98% yield as an orange yellow solid. Mp: 44-45 °C; $R_f = 0.1$ (EtOAc/cyclohexane 1:2). IR (ATR): 2967, 2809, 1706, 1434, 1386 cm^{-1} . ^1H NMR (400 MHz, DMSO- d_6) δ 0.86 (6H, t, $J = 7.2$ Hz), 2.44 (4H, q, $J = 7.2$ Hz), 2.59 (2H, t, $J = 6.8$ Hz), 3.63 (2H, t, $J = 6.8$ Hz), 7.81-7.88 (4H, m); ^{13}C NMR (100 MHz, DMSO- d_6) δ 12.0 (2CH₃), 35.8 (CH₂), 46.6 (2CH₂), 49.5 (CH₂), 123.0 (2CH_{arom}), 134.4 (2CH_{arom}), 131.6 (2C_{arom}), 167.9 (2CO).

4.1.5 2-(2-Morpholin-4-ylethyl)-1*H*-isoindole-1,3(2*H*)-dione (**6c**): prepared according to method A [11] in 80% yield as a beige solid. Mp: 139-140 °C; $R_f = 0.15$ (EtOAc/cyclohexane 1:2). IR (ATR): 2792, 1703, 1436, 1395 cm^{-1} . ^1H and ^{13}C NMR spectra were in accordance with published data [11].

4.1.6 2-(2-(*N*-Methylpiperazin-4-yl)ethyl)-1*H*-isoindole-1,3(2*H*)-dione (**6d**): prepared according to method B [12] in 73% yield as a yellow oil. $R_f = 0.1$ (EtOAc/cyclohexane 1:2). IR (ATR): 2946, 2796, 1702, 1437, 1400 cm^{-1} . ^1H NMR (400 MHz, DMSO- d_6) δ 2.09 (3H, s), 2.20-2.25 (4H, m), 2.27-2.40 (4H, m), 2.51 (2H, t, $J = 5.2$ Hz), 3.68 (2H, t, $J = 5.2$ Hz), 7.81-7.89 (4H, m). ^{13}C NMR (100 MHz, DMSO- d_6) δ 45.7 (CH₃), 35.0 (CH₂), 52.5 (2CH₂), 54.7 (2CH₂), 55.1 (CH₂), 123.0 (2CH_{arom}), 134.4 (2CH_{arom}), 131.6 (2C_{arom}), 167.8 (2CO).

4.1.7 2-(2-Piperidinylethyl)-1*H*-isoindole-1,3(2*H*)-dione (**6e**): prepared according to method B [12] in a quantitative yield as a brown solid. Mp: 75-76 °C; $R_f = 0.1$ (EtOAc/cyclohexane 1:2). IR (ATR): 2945, 1704, 1436, 1396 cm^{-1} . ^1H NMR (400 MHz, DMSO- d_6) δ 1.31-1.42 (6H, m), 2.34-2.37 (4H, m), 2.47 (2H, t, $J = 5.2$ Hz), 3.68 (2H, t, $J = 5.2$ Hz), 7.81-7.89 (4H, m); ^{13}C NMR (100 MHz, DMSO- d_6) δ 23.9 (CH₂), 25.6 (2CH₂), 35.1 (CH₂), 53.9 (2CH₂), 55.8 (CH₂), 123.0 (2CH_{arom}), 134.4 (2CH_{arom}), 131.6 (2C_{arom}), 167.8 (2CO).

4.1.8 2-(2-Pyrrolidinylethyl)-1*H*-isoindole-1,3(2*H*)-dione (**6f**): prepared according to method C [13] in 40% yield as a pale yellow solid. Mp: 101-102 °C; $R_f = 0.3$ (CH₂Cl₂/EtOH/Et₃N 9:1:1). IR (ATR): 2976, 2792, 1702, 1442, 1390 cm^{-1} . ^1H NMR (400 MHz, DMSO- d_6) δ 1.61-1.64 (4H, m), 2.44-2.48 (4H, m), 2.63 (2H, t, $J = 6.8$ Hz), 3.68 (2H, t, $J = 6.8$ Hz), 7.82-7.87 (4H, m); ^{13}C NMR (100 MHz, DMSO- d_6) δ 23.1 (2CH₂), 36.7, 53.2 (CH₂), 53.5 (2CH₂), 123.0 (2CH_{arom}), 134.4 (2CH_{arom}), 131.6 (2C_{arom}), 167.8 (2CO).

4.1.9 2-(3-Diethylaminopropyl)-1H-isoindole-1,3(2H)-dione (**6h**): prepared according to method C [13] in 93% yield. Mp and ¹H NMR data were in accordance with published data [16]. IR (ATR): 2968, 2805, 1705, 1394, 1366 cm⁻¹. ¹³C NMR (100 MHz, DMSO-*d*₆) δ 11.5 (2CH₃), 25.4, 36.1 (CH₂), 46.1 (2CH₂), 50.0 (CH₂), 122.9 (2CH_{arom}), 134.3 (2CH_{arom}), 131.7 (2C_{arom}), 167.9 (2CO).

4.1.10 2-(3-Morpholinylpropyl)-1H-isoindole-1,3(2H)-dione (**6i**): prepared according to method A [11] in 95% yield as a brown oil. R_f = 0.1 (EtOAc/cyclohexane 1:1). IR (ATR): 2954, 2813, 1702, 1395, 1361 cm⁻¹. ¹H NMR (400 MHz, DMSO-*d*₆) δ 1.73 (2H, quint, *J* = 6.8 Hz), 2.21-2.23 (4H, m), 2.30 (2H, t, *J* = 6.8 Hz), 3.32-3.41 (4H, m), 3.64 (2H, t, *J* = 6.8 Hz), 7.82-7.88 (4H, m); ¹³C NMR (100 MHz, DMSO-*d*₆) δ 24.0, 36.2 (CH₂), 53.2 (2CH₂), 56.0 (CH₂), 66.0 (2CH₂), 122.9 (2CH_{arom}), 134.2 (2CH_{arom}), 131.8 (2C_{arom}), 168.0 (2CO).

4.1.11 2-(3-(*N*-Methylpiperazin-4-yl)propyl)-1H-isoindole-1,3(2H)-dione (**6j**): prepared according to method B [12] in 81% yield as a brown solid. Mp: 62-63 °C. R_f = 0.1 (EtOAc/cyclohexane 1:1). IR (ATR): 2933, 2805, 1706, 1392, 1359 cm⁻¹. ¹H NMR (400 MHz, DMSO-*d*₆) δ 1.72 (2H, quint, *J* = 6.8 Hz), 1.97 (3H, s), 1.98-2.32 (8H, m), 2.29 (2H, t, *J* = 6.4 Hz), 3.63 (2H, t, *J* = 6.8 Hz), 7.82-7.88 (4H, m); ¹³C NMR (100 MHz, DMSO-*d*₆): 45.6 (CH₃), 24.1, 36.4 (CH₂), 52.6 (2CH₂), 54.4 (2CH₂), 55.7 (CH₂), 123.0 (2CH_{arom}), 134.2 (2CH_{arom}), 132.0 (2C_{arom}), 168.0 (2CO).

4.1.12 2-(3-Piperidinylpropyl)-1H-isoindole-1,3(2H)-dione (**6k**): prepared according to method A [11] in 82% yield. Mp, ¹H and ¹³C NMR were in accordance with published data [17]. R_f = 0.1 (EtOAc/cyclohexane 1:1). IR (ATR): 2932, 2771, 1697, 1395 cm⁻¹.

4.1.13 2-(3-Pyrrolidinylpropyl)-1H-isoindole-1,3(2H)-dione (**6l**): prepared according to method B [12] in quantitative yield as a brown oil. R_f = 0.1 (EtOAc/cyclohexane 1:1). IR (ATR): 2959, 2792, 1706, 1394, 1366 cm⁻¹. ¹H NMR (400 MHz, DMSO-*d*₆) δ 1.48-1.52 (4H, m), 1.73 (2H, quint, *J* = 6.8 Hz), 2.28-2.35 (4H, m), 2.40 (2H, t, *J* = 6.8 Hz), 3.63 (2H, t, *J* = 6.8 Hz), 7.81-7.88 (4H, m); ¹³C NMR (100 MHz, DMSO-*d*₆) δ 22.9 (2CH₂), 26.7, 36.2, 53.2 (CH₂), 53.4 (2CH₂), 122.8 (2CH_{arom}), 134.2 (2CH_{arom}), 131.8 (2C_{arom}), 168.0 (2CO).

General procedures for the preparation of compounds 7b-f and 7h-l.

To a solution of compounds **6b-l** (9.15 mmol) in 30 mL EtOH was added hydrazine monohydrate (36.6 mmol; 4 eq.) and the mixture was vigorously stirred under reflux for 24 h. The white solid

was filtered off and washed with EtOH. Filtrate was concentrated under vacuum to dryness and taken up with EtOAc. The solid residue was filtered again and filtrate was concentrated in vacuo to afford the desired products **7b-7l**. NH₂ signals are missing for all compounds in ¹H NMR spectra.

4.1.14 2-(N,N-(Diethylamino))ethanamine (7b): brown orange oil obtained in quantitative yield. IR (ATR): 3368-2500, 1445, 1371, 1068 cm⁻¹. ¹H NMR (400 MHz, DMSO-*d*₆) δ 0.93 (6H, t, *J* = 7.2 Hz), 2.34 (2H, t, *J* = 6.8 Hz), 2.43 (4H, q, *J* = 7.2 Hz), 2.53 (2H, t, *J* = 6.8 Hz); ¹³C NMR (100 MHz, DMSO-*d*₆) δ 11.9 (2CH₃), 39.7 (CH₂), 46.7 (2CH₂), 56.0 (CH₂).

4.1.15 2-Morpholin-4-ylethanamine (7c): orange oil obtained in 95% yield. ¹H, ¹³C NMR and mass spectra were in accordance with published data [11]. IR (ATR): 3568-2579, 1456, 1274, 1113 cm⁻¹.

4.1.16 2-(N-methylpiperazin-1-yl)ethanamine (7d): orange oil obtained in 56% yield. NMR spectra were in accordance with published data [18,19]. IR (ATR): 3631-2394, 1462, 1286, 1148 cm⁻¹.

4.1.17 2-(Piperidin-1-yl)ethanamine (7e): orange oil obtained in 43% yield. IR (ATR): 3566-2500, 1443, 1307, 1098 cm⁻¹. ¹H NMR (400 MHz, DMSO-*d*₆) δ 1.33-1.38 (2H, m), 1.44-1.51 (4H, m), 2.22 (2H, t, *J* = 6.4 Hz), 2.24-2.32 (4H, m), 2.58 (2H, t, *J* = 6.8 Hz); ¹³C NMR (100 MHz, DMSO-*d*₆) δ 24.2 (CH₂), 25.6 (2CH₂), 38.8 (CH₂), 54.3 (2CH₂), 61.9 (CH₂).

4.1.18 2-(Pyrrolidin-1-yl)ethanamine (7f): orange oil obtained in 82% yield. IR (ATR): 3579-2500, 1462, 1305, 1141 cm⁻¹. ¹H NMR (400 MHz, DMSO-*d*₆) δ 1.63-1.67 (4H, m), 2.37 (2H, t, *J* = 7.2 Hz), 2.36-2.41 (4H, m), 2.59 (2H, t, *J* = 7.2 Hz); ¹³C NMR (100 MHz, DMSO-*d*₆) δ 23.1 (2CH₂), 40.7 (CH₂), 53.7 (2CH₂), 59.2 (CH₂).

4.1.19 3-(N,N-Diethylamino)propanamine (7h): yellow oil obtained in 73% yield. IR (ATR): 3395-2710, 1467, 1381, 1202, 1069 cm⁻¹. ¹H NMR (400 MHz, DMSO-*d*₆) δ 0.92 (6H, t, *J* = 7.2 Hz), 1.42 (2H, quint, *J* = 7.2 Hz), 2.36 (2H, t, *J* = 7.2 Hz), 2.41 (4H, t, *J* = 7.2 Hz), 2.52 (2H, t, *J* = 6.8 Hz); ¹³C NMR (100 MHz, DMSO-*d*₆) δ 11.8 (2CH₃), 30.8, 40.1 (CH₂), 46.3 (2CH₂), 50.2 (CH₂).

4.1.20 3-(Morpholin-4-yl)propanamine (7i): brown oil obtained in 86% yield. IR (ATR): 3579-2618, 1448, 1307, 1271, 1113 cm⁻¹. ¹H NMR (400 MHz, DMSO-*d*₆) δ 1.47 (2H, quint, *J* = 7.2 Hz),

2.27 (2H, t, $J = 7.2$ Hz), 2.25-2.32 (4H, m), 2.53 (2H, t, $J = 7.2$ Hz), 3.55 (4H, t, $J = 4.4$ Hz); ^{13}C NMR (100 MHz, DMSO- d_6) δ 53.5 (3CH₂), 56.2 (CH₂), 66.3 (3CH₂).

4.1.21 3-(*N*-Methylpiperazin-1-yl)propanamine (**7j**): brown oil obtained in 86% yield. IR (ATR): 3461-2395, 1448, 1283, 1163 cm⁻¹. ^1H NMR (400 MHz, DMSO- d_6) δ 1.45 (2H, quint, $J = 5.6$ Hz), 2.13 (3H, s), 2.23-2.45 (8H, m), 2.26 (2H, t, $J = 5.6$ Hz), 2.52 (2H, t, $J = 5.2$ Hz); ^{13}C NMR (100 MHz, DMSO- d_6) δ 45.8 (CH₃), 30.3, 40.0 (CH₂), 52.8 (2CH₂), 54.8 (2CH₂), 55.8 (CH₂).

4.1.22 3-(Piperidin-1-yl)propanamine (**7k**): light brown oil obtained in 92% yield. Data in accordance with ^1H and ^{13}C NMR spectra already described [17]. IR (ATR): 3457-2511, 1561, 1468, 1442, 1304, 1156 cm⁻¹.

4.1.23 3-(Pyrrolidin-1-yl)propanamine (**7l**): brown orange oil obtained in 51% yield. IR (ATR): 3500-2579, 1591, 1460, 1350, 1141 cm⁻¹. ^1H NMR (400 MHz, DMSO- d_6) δ 1.48 (2H, quint, $J = 7.2$ Hz), 1.60-1.70 (4H, m), 2.30-2.43 (6H, m), 2.54 (2H, t, $J = 7.2$ Hz); ^{13}C NMR (100 MHz, DMSO- d_6) δ 23.0 (2CH₂), 32.5, 40.1, 53.6 (CH₂), 53.7 (2CH₂).

Synthetic procedures for the preparation of compounds 8a-l.

To a solution of primary amines **7a-l** (2 eq) in water (0.5 mol/L) was added *O*-methylisourea bisulfate (1 eq). Solution was stirred at 100 °C for 24 h. After concentration to dryness, ethanol was added and the residue was sonicated until apparition of a precipitate. In some difficult cases, the suspension in ethanol was stored overnight in a freezer and triturated with cold ethanol to get a powder. Addition of a few drops of diethylether was also occasionally needed to induce precipitation. The solids **8a-l** were collected by filtration, washed with ethanol and dried overnight under vacuum. Due to the hygroscopicity of isolated solids, no melting points were determined for these series. NH signals are missing for all compounds in ^1H NMR spectra.

4.1.24 1-(2-(*N,N*-Dimethylamino)ethyl)guanidine (**8a**): obtained as a white powder in 73% yield. IR (ATR): 3500-2344, 1694, 1637, 1480, 1061 cm⁻¹. ^1H NMR (400 MHz, CD₃OD/D₂O 9:1) δ 2.92 (6H, s), 3.36 (2H, t, $J = 6.0$ Hz), 3.66 (2H, t, $J = 6.0$ Hz); ^{13}C NMR (100 MHz, CD₃OD/D₂O 9:1) δ 44.0 (2CH₃), 37.5, 56.7 (CH₂), 158.3 (C).

4.1.25 *1-(2-(N,N-Diethylamino)ethyl)guanidine (8b)*: obtained as a white powder in 58% yield. IR (ATR): 3434-2342, 1620, 1396, 1028 cm⁻¹. ¹H NMR (400 MHz, CD₃OD/D₂O 9:1) δ 1.33 (6H, t, *J* = 7.2 Hz), 3.23 (4H, q, *J* = 7.2 Hz), 3.33 (2H, t, *J* = 6.4 Hz), 3.67 (2H, t, *J* = 6.4 Hz); ¹³C NMR (100 MHz, CD₃OD/D₂O 9:1) δ 9.0 (2CH₃), 37.6 (2CH₂), 38.5 (CH₂), 51.7 (CH₂), 158.7 (C).

4.1.26 *1-(2-(Morpholin-1-yl)ethyl)guanidine (8c)*: obtained as a beige powder in 45% yield. IR (ATR): 3552-2368, 1408, 1019 cm⁻¹. ¹H NMR (400 MHz, CD₃OD/D₂O 9:1) δ 2.75-2.85 (4H, m), 2.93 (2H, t, *J* = 6.4 Hz), 3.22 (2H, t, *J* = 6.4 Hz), 3.83 (4H, t, *J* = 4.8 Hz); ¹³C NMR (100 MHz, CD₃OD/D₂O 9:1) δ 36.4 (CH₂), 53.9 (2CH₂), 55.5 (CH₂), 66.9 (2CH₂), 158.4 (C).

4.1.27 *1-(2-(N-Methylpiperazin-1-yl)ethyl)guanidine (8d)*: obtained as a white powder in 73% yield. IR (ATR): 3447-2197, 1682, 1624, 1458, 1038 cm⁻¹. ¹H NMR (400 MHz, CD₃OD/D₂O 9:1) δ 2.73-2.79 (4H, m), 2.87 (3H, s), 2.86-2.93 (4H, m), 3.31-3.38 (4H, m); ¹³C NMR (100 MHz, CD₃OD/D₂O 9:1) δ 44.0 (CH₃), 39.5 (2CH₂), 50.7 (CH₂), 54.5 (2CH₂), 56.3 (CH₂), 158.6 (C).

4.1.28 *1-(2-(Piperidin-1-yl)ethyl)guanidine (8e)*: obtained as a white powder in 69% yield. IR (ATR): 3553-2237, 1687, 1626, 1457, 1038 cm⁻¹. ¹H NMR (400 MHz, CD₃OD/D₂O 9:1) δ 2.00-2.42 (6H, m), 2.84-3.75 (4H, m), 3.36 (4H, t, *J* = 6.4 Hz); ¹³C NMR (100 MHz, CD₃OD/D₂O 9:1) δ 23.9 (2CH₂), 26.1, 39.4, 53.2 (CH₂), 55.1 (2CH₂), 158.3 (C).

4.1.29 *1-(2-(Pyrrolidin-1-yl)ethyl)guanidine (8f)*: obtained as a white powder in 66% yield. IR (ATR): 3553-2237, 1633, 1407, 1034 cm⁻¹. ¹H NMR (400 MHz, CD₃OD/D₂O 9:1) δ 2.10-2.13 (4H, m), 3.31-3.44 (4H, m), 3.55 (2H, t, *J* = 6.4 Hz), 3.66 (2H, t, *J* = 6.0 Hz); ¹³C NMR (100 MHz, CD₃OD/D₂O 9:1) δ 23.9 (2CH₂), 38.6 (CH₂), 49.2 (2CH₂), 55.4 (CH₂), 158.5 (C).

4.1.30 *1-(3-(N,N-Dimethylamino)propyl)guanidine (8g)*: obtained as a white powder in 88% yield. IR (ATR): 3605-2395, 1678, 1629, 1485, 1075 cm⁻¹. ¹H NMR (400 MHz, CD₃OD/D₂O 9:1) δ 2.06 (2H, quint, *J* = 8.0 Hz), 2.89 (6H, s), 3.20 (2H, t, *J* = 8.0 Hz), 3.32 (2H, t, under solvent signal); ¹³C NMR (100 MHz, CD₃OD/D₂O 9:1) δ 43.7 (2CH₃), 24.8, 39.2, 55.9 (CH₂), 158.1 (C).

4.1.31 *1-(3-(N,N-Diethylamino)propyl)guanidine (8h)*: obtained as a white powder in 62% yield. IR (ATR): 3498-2395, 1689, 1637, 1483, 1038 cm⁻¹. ¹H NMR (400 MHz, CD₃OD/D₂O 9:1) δ 1.31 (6H, t, *J* = 7.2 Hz), 1.98-2.08 (2H, m), 3.15-3.26 (2H, m), 3.22 (4H, q, *J* = 7.2 Hz), 3.28-3.33 (2H,

m); ^{13}C NMR (100 MHz, $\text{CD}_3\text{OD}/\text{D}_2\text{O}$ 9:1) δ 9.0 (2 CH_3), 24.3, 39.4 (CH_2), 48.1 (2 CH_2), 50.2 (CH_2), 158.2 (C).

4.1.32 *1-(3-(Morpholin-1-yl)propyl)guanidine (8i)*: obtained as a beige powder in 42% yield. IR (ATR): 3605-2184, 1684, 1633, 1480, 1042 cm^{-1} . ^1H NMR (400 MHz, $\text{CD}_3\text{OD}/\text{D}_2\text{O}$ 9:1) δ 2.00-2.18 (2H, m), 3.18-3.55 (8H, m), 3.89-4.07 (4H, m); ^{13}C NMR (100 MHz, $\text{CD}_3\text{OD}/\text{D}_2\text{O}$ 9:1) δ 23.8, 39.3 (CH_2), 52.9 (2 CH_2), 55.3 (CH_2), 64.9 (2 CH_2), 158.3 (C).

4.1.33 *1-(3-(N-Methylpiperazin-1-yl)propyl)guanidine (8j)*: obtained as a white powder in 54% yield. IR (ATR): 3433-2574, 1685, 1641, 1474, 1027 cm^{-1} . ^1H NMR (400 MHz, $\text{CD}_3\text{OD}/\text{D}_2\text{O}$ 9:1) δ 1.86 (2H, quint, $J = 7.2$ Hz), 2.64-2.72 (2H, m), 2.75 (3H, s), 2.74-3.32 (8H, m), 3.25 (2H, t, $J = 7.2$ Hz); ^{13}C NMR (100 MHz, $\text{CD}_3\text{OD}/\text{D}_2\text{O}$ 9:1) δ 44.1 (CH_3), 25.8 (CH_2), 39.9 (2 CH_2), 51.0, 53.8 (CH_2), 54.8 (2 CH_2), 158.2 (C).

4.1.34 *1-(3-(Piperidin-1-yl)propyl)guanidine (8k)*: obtained as a white powder in 83% yield. IR (ATR): 3316-2737, 1680, 1629, 1389, 1028 cm^{-1} . ^1H NMR (400 MHz, $\text{CD}_3\text{OD}/\text{D}_2\text{O}$ 9:1) δ 1.71-2.00 (6H, m), 2.07 (2H, quint, $J = 7.2$ Hz), 2.84-2.96 (2H, m), 3.12-3.17 (2H, m), 3.29 (2H, t, $J = 7.2$ Hz), 3.46-3.59 (2H, m); ^{13}C NMR (100 MHz, $\text{CD}_3\text{OD}/\text{D}_2\text{O}$ 9:1) δ 22.4 (CH_2), 23.9 (2 CH_2), 24.2, 39.4 (CH_2), 54.3 (2 CH_2), 55.0 (CH_2), 158.1 (C).

4.1.35 *1-(3-(Pyrrolidin-1-yl)propyl)guanidine (8l)*: obtained as a white powder in 74% yield. IR (ATR): 3552-2118, 1674, 1632, 1479, 1027 cm^{-1} . ^1H NMR (400 MHz, $\text{CD}_3\text{OD}/\text{D}_2\text{O}$ 9:1) δ 1.45-1.80 (2H, m), 1.60-2.34 (4H, m), 2.69-3.78 (6H, m), 3.69 (2H, t, $J = 6.4$ Hz); ^{13}C NMR (100 MHz, $\text{CD}_3\text{OD}/\text{D}_2\text{O}$ 9:1) δ 22.5 (CH_2), 23.8 (2 CH_2), 37.0 (CH_2), 54.7 (2 CH_2), 56.1 (CH_2), 158.4 (C).

Synthetic procedure for the preparation of compounds 9a-m.

To a solution of previously described compound **1** (50 mg, 0.211 mmol, 1.1 eq) in 0.8 mL of *N,N*-dimethylacetamide were successively added the guanidinium salts **8a-m** (1 eq) and potassium carbonate (87 mg, 0.633 mmol, 3.3 eq). The suspension was heated at 70 °C for 25 to 150 min. Reaction mixture was filtered over Celite and washed with EtOAc. After evaporation of the solvents, the crude residue was purified by column chromatography using a mixture of $\text{CH}_2\text{Cl}_2/\text{NH}_3$ 7N solution in MeOH from 98:2 to 96:4.

For each compound, two rotamers are observed by NMR but only the major one is described.

4.1.36 *N*-(2-(*N,N*-Dimethylamino)ethyl)-10-nitropyrido[3,4-*g*]quinazolin-2-amine (**9a**): 90 min reaction time, obtained as an orange yellow powder in 14% yield. Mp: 224-225 °C; $R_f = 0.35$ ($\text{CH}_2\text{Cl}_2/\text{NH}_3$ 7N solution in MeOH 96:4). IR (ATR): 3266-2359, 1581, 1521, 1342, 1186 cm^{-1} . ^1H NMR (400 MHz, $\text{DMSO-}d_6$) δ 2.22 (6H, s), 2.45-2.55 (2H, m, under solvent signal), 3.46-3.52 (2H, m), 7.57 (1H, d, $J = 6.0$ Hz), 8.51 (1H, t, $J = 6.4$ Hz, NH), 8.58 (1H, d, $J = 6.4$ Hz), 8.98 (1H, s), 9.535 (1H, s), 9.543 (1H, s); ^{13}C NMR (100 MHz, $\text{DMSO-}d_6$) δ 44.8 (2 CH_3), 38.5, 57.1 (CH_2), 112.3, 134.3, 146.3, 155.0, 165.1 (CH_{arom}), 119.9, 122.0, 128.7, 136.5, 141.3, 159.5 (C_{arom}). HRMS (ESI+) calcd for $\text{C}_{15}\text{H}_{17}\text{N}_6\text{O}_2$ ($\text{M}+\text{H}$) $^+$ 313.1413, found 313.1405. HPLC: purity > 96%, $\lambda = 240$ nm, $t_{\text{R}} = 18.5$ min.

4.1.37 *N*-(2-(*N,N*-Diethylamino)ethyl)-10-nitropyrido[3,4-*g*]quinazolin-2-amine (**9b**): 25 min reaction time, obtained as an orange yellow powder in 14% yield. Mp: 134-135 °C; $R_f = 0.35$ ($\text{CH}_2\text{Cl}_2/\text{NH}_3$ 7N solution in MeOH 96:4). IR (ATR): 3447-2342, 1584, 1525, 1355 cm^{-1} . ^1H NMR (400 MHz, $\text{DMSO-}d_6$) δ 0.97 (6H, t, $J = 6,8$ Hz), 2.40-2.78 (6H, m), 3.40-3.47 (2H, m), 7.56 (1H, d, $J = 6.4$ Hz), 8.49 (1H, t, $J = 6.4$ Hz, NH), 8.58 (1H, d, $J = 6.4$ Hz), 8.98 (1H, s), 9.53 (1H, s), 9.54 (1H, s); ^{13}C NMR (100 MHz, $\text{DMSO-}d_6$) δ 11.9 (2 CH_3), 1 CH_2 under solvent signal, 46.8 (2 CH_2), 50.6 (CH_2), 112.3, 134.2, 146.2, 155.0, 165.0 (CH_{arom}), 119.9, 122.0, 128.7, 136.5, 141.4, 159.5 (C_{arom}). HRMS (ESI+) calcd for $\text{C}_{17}\text{H}_{21}\text{N}_6\text{O}_2$ ($\text{M}+\text{H}$) $^+$ 341.1721, found 341.1712.

4.1.38 *N*-(2-Morpholinoethyl)-10-nitropyrido[3,4-*g*]quinazolin-2-amine (**9c**): 140 min reaction time, obtained as an orange powder in 12% yield. Mp: 211-212 °C; $R_f = 0.25$ (acetone). IR (ATR): 3595-2543, 1584, 1527, 1361, 1304, 1113 cm^{-1} . ^1H NMR (400 MHz, $\text{DMSO-}d_6$) δ 2.41-2.58 (6H, m), 3.50 (2H, t, $J = 6.4$ Hz), 3.54 (4H, t, $J = 4.4$ Hz), 7.57 (1H, d, $J = 6.4$ Hz), 8.52 (1H, t, $J = 5.6$ Hz, NH), 8.58 (1H, d, $J = 6.0$ Hz), 8.98 (1H, s), 9.537 (1H, s), 9.543 (1H, s); ^{13}C NMR (100 MHz, $\text{DMSO-}d_6$) δ 37.9 (CH_2), 53.3 (2 CH_2), 56.7 (CH_2), 66.2 (2 CH_2), 112.3, 134.3, 146.3, 155.0, 165.1 (CH_{arom}), 119.9, 122.0, 128.7, 136.5, 141.4, 159.5 (C_{arom}). HRMS (ESI+) calcd for $\text{C}_{17}\text{H}_{19}\text{N}_6\text{O}_3$ ($\text{M}+\text{H}$) $^+$ 355.1513, found 355.1508.

4.1.39 *N*-(2-(*N*-Methylpiperazin-1-yl)ethyl)-10-nitropyrido[3,4-*g*]quinazolin-2-amine (**9d**): 45 min reaction time, obtained as an orange yellow powder in 15% yield. Mp: 177-178 °C; $R_f = 0.20$ ($\text{CH}_2\text{Cl}_2/\text{NH}_3$ 7N solution in MeOH 96:4). IR (ATR): 3355-2158, 1583, 1523, 1347, 1153 cm^{-1} . ^1H NMR (400 MHz, $\text{DMSO-}d_6$) δ 2.12 (3H, s), 2.20-2.55 (8H, m), 2.54 (2H, t, $J = 7.2$ Hz), 3.46-3.52

(2H, m), 7.57 (1H, d, $J = 6.0$ Hz), 8.48 (1H, t, $J = 6.0$ Hz, NH), 8.58 (1H, d, $J = 6.0$ Hz), 8.98 (1H, s), 9.53 (1H, s), 9.54 (1H, s); ^{13}C NMR (100 MHz, DMSO- d_6) δ 45.7 (CH₃), 38.3 (CH₂), 52.6 (2CH₂), 54.7 (2CH₂), 56.2 (CH₂), 112.4, 134.3, 146.3, 155.0, 165.1 (CH_{arom}), 119.9, 122.0, 128.7, 136.5, 141.4, 159.5 (C_{arom}). HRMS (ESI+) calcd for C₁₈H₂₂N₇O₂ (M+H)⁺ 368.1830, found 368.1826.

4.1.40 *N*-(2-(Piperidin-1-yl)ethyl)-10-nitropyrido[3,4-*g*]quinazolin-2-amine (**9e**): 45 min reaction time, obtained as an orange powder in 30% yield. Mp: 125-126 °C; $R_f = 0.20$ (CH₂Cl₂/NH₃ 7N solution in MeOH 96:4). IR (ATR): 3421-2355, 1583, 1525, 1342, 1123 cm⁻¹. ^1H NMR (400 MHz, DMSO- d_6) δ 1.34-1.38 (2H, m), 1.41-1.50 (4H, m), 2.25-2.60 (6H, m), 3.46-3.52 (2H, m), 7.57 (1H, d, $J = 6.0$ Hz), 8.48 (1H, t, $J = 6.0$ Hz, NH), 8.58 (1H, d, $J = 6.0$ Hz), 8.98 (1H, s), 9.53 (1H, s), 9.54 (1H, s); ^{13}C NMR (100 MHz, DMSO- d_6) δ 24.0 (CH₂), 25.6 (2CH₂), 53.6 (CH₂), 54.1 (2CH₂), 56.9 (CH₂), 112.3, 134.2, 146.3, 155.0, 165.0 (CH_{arom}), 119.9, 122.0, 128.8, 135.4, 141.4, 159.5 (C_{arom}). HRMS (ESI+) calcd for C₁₈H₂₁N₆O₂ (M+H)⁺ 353.1721, found 353.1729.

4.1.41 *N*-(2-(Pyrrolidin-1-yl)ethyl)-10-nitropyrido[3,4-*g*]quinazolin-2-amine (**9f**): 25 min reaction time, obtained as an orange powder in 15% yield. Mp: 158-159 °C; $R_f = 0.20$ (CH₂Cl₂/NH₃ 7N solution in MeOH 96:4). IR (ATR): 3434-2342, 1583, 1524, 1346, 1151 cm⁻¹. ^1H NMR (400 MHz, DMSO- d_6) δ 1.60-1.75 (4H, m), 2.40-2.60 (6H, m, under solvent signal), 3.46-3.54 (2H, m), 7.57 (1H, d, $J = 6.4$ Hz), 8.55 (1H, t, $J = 6.8$ Hz, NH), 8.58 (1H, d, $J = 6.0$ Hz), 8.98 (1H, s), 9.536 (1H, s), 9.544 (1H, s); ^{13}C NMR (100 MHz, DMSO- d_6) δ 23.2 (2CH₂), 1 CH₂ under solvent signal, 53.6 (2CH₂), 54.0 (CH₂), 112.3, 134.3, 146.3, 155.0, 165.1 (CH_{arom}), 119.9, 122.0, 128.8, 136.5, 141.4, 159.5 (C_{arom}). HRMS (ESI+) calcd for C₁₇H₁₉N₆O₂ (M+H)⁺ 339.1564, found 339.1557.

4.1.42 *N*-(3-(*N,N*-Dimethylamino)propyl)-10-nitropyrido[3,4-*g*]quinazolin-2-amine (**9g**): 45 min reaction time, obtained as an orange yellow powder in 16% yield. $R_f = 0.15$ (CH₂Cl₂/NH₃ 7N solution in MeOH 97:3). Mp: 136-137 °C; IR (ATR): 3375-2453, 1586, 1521, 1355, 1294 cm⁻¹. ^1H NMR (400 MHz, DMSO- d_6) δ 1.74 (2H, quint, $J = 7.2$ Hz), 2.14 (6H, s), 2.29 (2H, t, $J = 7.2$ Hz), 3.35-3.40 (2H, m), 7.56 (1H, d, $J = 6.8$ Hz), 8.57 (1H, d, $J = 6.4$ Hz), 8.65 (1H, t, $J = 5.6$ Hz, NH), 8.97 (1H, s), 9.52 (1H, s), 9.54 (1H, s); ^{13}C NMR (100 MHz, DMSO- d_6) δ 45.1 (2CH₃), 26.0, 56.8 (CH₂), 112.3, 134.1, 146.2, 154.9, 164.9 (CH_{arom}), 119.9, 122.0, 128.7, 136.5, 141.4, 159.4 (C_{arom}). The missing CH₂ was under the solvent signal. HRMS (ESI+) calcd for C₁₆H₁₉N₆O₂ (M+H)⁺ 327.1569, found 327.1540.

4.1.43 *N*-(3-(*N,N*-Diethylamino)propyl)-10-nitropyrido[3,4-*g*]quinazolin-2-amine (**9h**): 45 min reaction time, obtained as a ochre yellow powder in 19% yield. Mp: 151-152 °C; $R_f = 0.20$ ($\text{CH}_2\text{Cl}_2/\text{NH}_3$ 7N solution in MeOH 96:4). IR (ATR): 3316-2355, 1584, 1526, 1355, 1205 cm^{-1} . ^1H NMR (400 MHz, $\text{DMSO-}d_6$) δ 0.95 (6H, t, $J = 7.2$ Hz), 1.73 (2H, quint, $J = 7.2$ Hz), 2.40-2.61 (6H, m), 3.35-3.42 (2H, m), 7.56 (1H, d, $J = 6.4$ Hz), 8.57 (1H, d, $J = 6.0$ Hz), 8.68 (1H, t, $J = 6.0$ Hz, NH), 8.97 (1H, s), 9.52 (1H, s), 9.54 (1H, s); ^{13}C NMR (100 MHz, $\text{DMSO-}d_6$) δ 11.6 (2 CH_3), 25.5 (CH_2), 46.20 (2 CH_2), 46.24 (CH_2), 50.1 (CH_2), 112.3, 134.1, 146.2, 155.0, 165.0 (CH_{arom}), 119.9, 121.9, 128.7, 136.5, 141.4, 159.4 (C_{arom}). HRMS (ESI+) calcd for $\text{C}_{18}\text{H}_{23}\text{N}_6\text{O}_2$ ($\text{M}+\text{H}$) $^+$ 355.1877, found 355.1881.

4.1.44 *N*-(3-Morpholinopropyl)-10-nitropyrido[3,4-*g*]quinazolin-2-amine (**9i**): 45 min reaction time, obtained as an orange yellow powder in 24% yield. Mp: 209-210 °C; $R_f = 0.20$ ($\text{CH}_2\text{Cl}_2/\text{NH}_3$ 7N solution in MeOH 96:4). IR (ATR): 3289-2342, 1583, 1530, 1357, 1144 cm^{-1} . ^1H NMR (400 MHz, $\text{DMSO-}d_6$) δ 1.77 (2H, quint, $J = 6.0$ Hz), 2.30-2.40 (6H, m), 3.39-3.44 (2H, m), 3.54-3.59 (4H, m), 7.56 (1H, d, $J = 4.8$ Hz), 8.57 (1H, d, $J = 4.8$ Hz), 8.65 (1H, t, $J = 4.8$ Hz, NH), 8.97 (1H, s), 9.52 (1H, s), 9.54 (1H, s); ^{13}C NMR (100 MHz, $\text{DMSO-}d_6$) δ 24.9, 39.4 (CH_2), 53.2 (2 CH_2), 55.9 (CH_2), 66.3 (2 CH_2), 112.3, 134.1, 146.3, 155.0, 165.0 (CH_{arom}), 119.9, 121.9, 128.7, 136.5, 141.4, 159.5 (C_{arom}). HRMS (ESI+) calcd for $\text{C}_{18}\text{H}_{21}\text{N}_6\text{O}_3$ ($\text{M}+\text{H}$) $^+$ 369.1670, found 369.1667.

4.1.45 *N*-(3-(*N*-Methylpiperazin-1-yl)propyl)-10-nitropyrido[3,4-*g*]quinazolin-2-amine (**9j**): 60 min reaction time, obtained as an orange yellow powder in 17% yield. Mp: 192-193 °C; $R_f = 0.20$ ($\text{CH}_2\text{Cl}_2/\text{NH}_3$ 7N solution in MeOH 96:4). IR (ATR): 3289-2342, 1584, 1524, 1345, 1141 cm^{-1} . ^1H NMR (400 MHz, $\text{DMSO-}d_6$) δ 1.75 (2H, quint, $J = 5.2$ Hz), 2.13 (2H, t, $J = 5.2$ Hz), 2.16 (3H, s), 2.17-2.60 (8H, m), 3.37-3.44 (2H, m), 7.57 (1H, d, $J = 5.2$ Hz), 8.57 (1H, d, $J = 4.8$ Hz), 8.64 (1H, t, $J = 4.8$ Hz, NH), 8.97 (1H, s), 9.52 (1H, s), 9.54 (1H, s); ^{13}C NMR (100 MHz, $\text{DMSO-}d_6$) δ 45.7 (CH_3), 25.3 (CH_2), 1 CH_2 under solvent signal, 52.6 (2 CH_2), 54.8 (2 CH_2), 55.5 (CH_2), 112.3, 134.1, 146.2, 155.0, 165.0 (CH_{arom}), 119.9, 121.9, 128.7, 136.5, 141.4, 159.4 (C_{arom}). HRMS (ESI+) calcd for $\text{C}_{19}\text{H}_{24}\text{N}_7\text{O}_2$ ($\text{M}+\text{H}$) $^+$ 382.1986, found 382.1987. HPLC: purity > 95%, $\lambda = 240$ nm, $t_R = 18.3$ min.

4.1.46 *N*-(3-(Piperidin-1-yl)propyl)-10-nitropyrido[3,4-*g*]quinazolin-2-amine (**9k**): 45 min reaction time, obtained as a brown orange powder in 22% yield. Mp: 185-186 °C; $R_f = 0.20$ ($\text{CH}_2\text{Cl}_2/\text{NH}_3$

7N solution in MeOH 97:3). IR (ATR): 3289-2316, 1587, 1530, 1359, 1152 cm^{-1} . ^1H NMR (400 MHz, $\text{DMSO-}d_6$) δ 1.34-1.52 (6H, m), 1.76 (2H, quint, $J = 6.8$ Hz), 2.31-2.36 (6H, m), 3.36-3.42 (2H, m), 7.56 (1H, d, $J = 6.0$ Hz), 8.57 (1H, d, $J = 6.0$ Hz), 8.67 (1H, t, $J = 5.2$ Hz, NH), 8.97 (1H, s), 9.52 (1H, s), 9.53 (1H, s); ^{13}C NMR (100 MHz, $\text{DMSO-}d_6$) δ 24.1, 25.2 (CH_2), 25.6 (2CH_2), 1CH_2 under solvent signal, 54.0 (2CH_2), 56.3 (CH_2), 112.3, 134.1, 146.3, 155.0, 165.0 (CH_{arom}), 119.9, 121.9, 128.7, 136.5, 141.4, 159.4 (C_{arom}). HRMS (ESI+) calcd for $\text{C}_{19}\text{H}_{23}\text{N}_6\text{O}_2$ ($\text{M}+\text{H}$) $^+$ 367.1877, found 367.1882.

4.1.47 N-(3-(Pyrrolidin-1-yl)propyl)-10-nitropyrido[3,4-g]quinazolin-2-amine (9l): 45 min reaction time, obtained as an orange yellow powder in 15% yield. Mp: 172-173 $^{\circ}\text{C}$; $R_f = 0.20$ ($\text{CH}_2\text{Cl}_2/\text{NH}_3$ 7N solution in MeOH 97:3). IR (ATR): 3368-2342, 1583, 1525, 1349, 1147 cm^{-1} . ^1H NMR (400 MHz, $\text{DMSO-}d_6$) δ 1.68-1.72 (4H, m), 1.78 (2H, quint, $J = 6.8$ Hz), 2.40-2.52 (6H, m), 3.38-3.45 (2H, m), 7.56 (1H, d, $J = 6.0$ Hz), 8.57 (1H, d, $J = 6.4$ Hz), 8.65 (1H, t, $J = 5.2$ Hz, NH), 8.97 (1H, s), 9.52 (1H, s), 9.53 (1H, s); ^{13}C NMR (100 MHz, $\text{DMSO-}d_6$) δ 23.1 (2CH_2), 27.3, 39.6, 53.4 (CH_2), 53.6 (2CH_2), 112.3, 134.2, 146.3, 155.0, 165.0 (CH_{arom}), 119.9, 121.9, 128.7, 136.5, 141.4, 159.5 (C_{arom}). HRMS (ESI+) calcd for $\text{C}_{18}\text{H}_{21}\text{N}_6\text{O}_2$ ($\text{M}+\text{H}$) $^+$ 353.1721, found 353.1722.

4.1.48 N-Methyl-10-nitropyrido[3,4-g]quinazolin-2-amine (9m): 45 min reaction time, obtained as a yellow powder in 12% yield. Mp: 224-225 $^{\circ}\text{C}$; $R_f = 0.45$ ($\text{CH}_2\text{Cl}_2/\text{NH}_3$ 7N solution in MeOH 97:3). IR (ATR): 3344-2502, 1586, 1508, 1382, 1351, 1295 cm^{-1} . ^1H NMR (400 MHz, $\text{DMSO-}d_6$) δ 2.93 (3H, d, $J = 4.8$ Hz), 7.57 (1H, d, $J = 6.4$ Hz), 8.51-8.56 (1H, m, NH), 8.59 (1H, d, $J = 6.4$ Hz), 8.99 (1H, s), 9.53 (1H, s), 9.55 (1H, s); ^{13}C NMR (100 MHz, $\text{DMSO-}d_6$) δ 27.9 (CH_3), 112.3, 134.2, 146.3, 155.0, 164.9 (CH_{arom}), 119.9, 122.0, 128.8, 136.6, 141.4, 159.9 (C_{arom}). HRMS (ESI+) calcd for $\text{C}_{12}\text{H}_{10}\text{N}_5\text{O}_2$ ($\text{M}+\text{H}$) $^+$ 256.0834, found 256.0815. HPLC: purity > 98%, $\lambda = 240$ nm, $t_R = 18.9$ min.

Synthetic procedure for the preparation of compounds 10a-m.

To a solution of nitro derivatives **9a-m** in anhydrous CH_2Cl_2 (0.04 mol/L) was added 6 mg/mmol of 10% Pd/C at room temperature. The suspension was stirred in the dark under 1 atm of H_2 until completion of the reaction (4 to 40 hours). The reaction mixture was filtered over Celite in a Pasteur pipette, washed with CH_2Cl_2 and evaporated. The product was not purified. Two rotamers were observed by NMR, but only the major one is described.

4.1.49 *N*2-(2-(*N,N*-Dimethylamino)ethyl)pyrido[3,4-*g*]quinazoline-2,10-diamine (**10a**): 18 h reaction time, obtained as a red oil in 65% yield. $R_f = 0.35$ ($\text{CH}_2\text{Cl}_2/\text{NH}_3$ 7N solution in MeOH 96:4). IR (ATR): 3500-2407, 1607, 1575, 1372, 1291 cm^{-1} . ^1H NMR (400 MHz, $\text{DMSO-}d_6$) δ 2.30 (6H, s), 2.45-2.65 (2H, m, under solvent signal), 3.60-3.65 (2H, m), 6.31 (2H, br s, NH_2), 7.40 (1H, br s, NH), 7.84 (1H, s), 7.99 (1H, d, $J = 6.0$ Hz), 8.22 (1H, d, $J = 6.0$ Hz), 9.24 (1H, s), 9.33 (1H, s); ^{13}C NMR (100 MHz, $\text{DMSO-}d_6$) δ 45.0 (2 CH_3), 29.0, 38.6 (CH_2), 113.5, 115.3, 139.5, 154.7, 164.4 (CH_{arom}), 119.1, 121.3, 124.4, 136.1, 142.5, 157.2 (C_{arom}). HRMS (ESI+) calcd for $\text{C}_{15}\text{H}_{19}\text{N}_6$ ($\text{M}+\text{H}$) $^+$ 283.1666, found 283.1665.

4.1.50 *N*2-(2-(*N,N*-Diethylamino)ethyl)pyrido[3,4-*g*]quinazoline-2,10-diamine (**10b**): 24 h reaction time, obtained as a red oil in 82% yield. $R_f = 0.15$ ($\text{CH}_2\text{Cl}_2/\text{NH}_3$ 7N solution in MeOH 96:4). IR (ATR): 3531-2189, 1606, 1574, 1372, 1028 cm^{-1} . ^1H NMR (400 MHz, $\text{DMSO-}d_6$) δ 1.00 (6H, t, $J = 7.2$ Hz), 2.57 (4H, q, $J = 7.2$ Hz), 2.62-2.71 (2H, m), 3.50-3.57 (2H, m), 6.28 (2H, br s, NH_2), 7.39 (1H, br s, NH), 7.83 (1H, s), 7.96 (1H, d, $J = 6.0$ Hz), 8.22 (1H, d, $J = 6.4$ Hz), 9.22 (1H, s), 9.31 (1H, s); ^{13}C NMR (100 MHz, $\text{DMSO-}d_6$) δ 11.9 (2 CH_3), 1 CH_2 under solvent signal, 46.7 (2 CH_2), 50.5 (CH_2), 113.7, 115.3, 139.6, 154.7, 164.4 (CH_{arom}), 119.2, 121.3, 124.4, 136.0, 142.3, 159.5 (C_{arom}). HRMS (ESI+) calcd for $\text{C}_{17}\text{H}_{23}\text{N}_6$ ($\text{M}+\text{H}$) $^+$ 311.1979, found 311.1979.

4.1.51 *N*2-(2-(Morpholin-1-yl)ethyl)pyrido[3,4-*g*]quinazoline-2,10-diamine (**10c**): 24 h reaction time, obtained as a red oil in 59% yield. $R_f = 0.20$ ($\text{CH}_2\text{Cl}_2/\text{NH}_3$ 7N solution in MeOH 96:4). IR (ATR): 3465-2449, 1606, 1575, 1372, 1112 cm^{-1} . ^1H NMR (400 MHz, $\text{DMSO-}d_6$) δ 2.50-2.62 (6H, m), 3.56-3.65 (6H, m), 6.30 (2H, br s, NH_2), 7.42 (1H, br s, NH), 7.83 (1H, s), 7.99 (1H, d, $J = 6.4$ Hz), 8.21 (1H, d, $J = 6.4$ Hz), 9.22 (1H, s), 9.32 (1H, s); ^{13}C NMR (100 MHz, $\text{DMSO-}d_6$) δ 24.4, 38.0 (CH_2), 53.4 (2 CH_2), 66.2 (2 CH_2), 113.6, 115.3, 139.5, 154.7, 164.9 (CH_{arom}), 119.1, 121.2, 124.4, 136.1, 142.2, 159.7 (C_{arom}). HRMS (ESI+) calcd for $\text{C}_{17}\text{H}_{21}\text{N}_6\text{O}$ ($\text{M}+\text{H}$) $^+$ 325.1771, found 325.1770.

4.1.52 *N*2-(2-(*N*-Methylpiperazin-1-yl)ethyl)pyrido[3,4-*g*]quinazoline-2,10-diamine (**10d**): 24 h reaction time, obtained as a red oil in 64% yield. $R_f = 0.15$ ($\text{CH}_2\text{Cl}_2/\text{NH}_3$ 7N solution in MeOH 96:4). IR (ATR): 3552-2598, 1608, 1576, 1374, 1147 cm^{-1} . ^1H NMR (400 MHz, $\text{DMSO-}d_6$) δ 2.14 (3H, s), 2.25-2.60 (10H, m), 3.56-3.62 (2H, m), 6.30 (2H, br s, NH_2), 7.38 (1H, br s, NH), 7.82 (1H, s), 7.99 (1H, d, $J = 7.2$ Hz), 8.21 (1H, d, $J = 7.2$ Hz), 9.22 (1H, s), 9.32 (1H, s); ^{13}C NMR (100 MHz, $\text{DMSO-}d_6$) δ 45.7 (CH_3), 38.4 (CH_2), 52.7 (2 CH_2), 54.7 (2 CH_2), 56.3 (CH_2), 113.6, 115.4,

139.6, 154.7, 164.7 (CH_{arom}), 120.0, 121.3, 124.4, 136.1, 142.2, 159.6 (C_{arom}). HRMS (ESI+) calcd for C₁₈H₂₄N₇ (M+H)⁺ 338.2088, found 338.2087.

4.1.53 *N*2-(2-(Piperidin-1-yl)ethyl)pyrido[3,4-*g*]quinazoline-2,10-diamine (**10e**): 24 h reaction time, obtained as a red oil in 44% yield. R_f = 0.15 (CH₂Cl₂/NH₃ 7N solution in MeOH 97:3). IR (ATR): 3482-2362, 1607, 1574, 1303, 1128 cm⁻¹. ¹H NMR (400 MHz, DMSO-*d*₆): 1.34-1.62 (6H, m), 2.25-2.60 (6H, m), 3.56-3.65 (2H, m), 6.31 (2H, br s, NH₂), 7.37 (1H, br s, NH), 7.83 (1H, s), 8.00 (1H, d, *J* = 5.6 Hz), 8.22 (1H, d, *J* = 5.6 Hz), 9.23 (1H, s), 9.33 (1H, s); ¹³C NMR (100 MHz, DMSO-*d*₆): 23.7 (CH₂), 25.4 (2CH₂), 38.2 (CH₂), 1CH₂ under solvent signal, 54.1 (2CH₂), 113.6, 115.4, 139.6, 154.7, 164.6 (CH_{arom}), 119.2, 121.3, 124.5, 136.2, 142.3, 159.0 (C_{arom}). HRMS (ESI+) calcd for C₁₈H₂₃N₆ (M+H)⁺ 323.1979, found 323.1978.

4.1.54 *N*2-(2-(Pyrrolidin-1-yl)ethyl)pyrido[3,4-*g*]quinazoline-2,10-diamine (**10f**): 24 h reaction time, obtained as a red oil in 98% yield. R_f = 0.15 (CH₂Cl₂/NH₃ 7N solution in MeOH 96:4). IR (ATR): 3531-2189, 1606, 1575, 1365, 1029 cm⁻¹. ¹H NMR (400 MHz, DMSO-*d*₆) δ 1.74-1.94 (4H, m), 2.40-2.75 (6H, m), 3.68-3.85 (2H, m), 6.41 (2H, br s, NH₂), 7.66 (1H, br s, NH), 7.85 (1H, s), 8.03 (1H, d, *J* = 6.4 Hz), 8.24 (1H, d, *J* = 6.0 Hz), 9.25 (1H, s), 9.37 (1H, s); ¹³C NMR (100 MHz, DMSO-*d*₆) δ 22.7 (2CH₂), 29.3, 46.2 (CH₂), 53.3 (2CH₂), 113.3, 115.4, 139.5, 154.7, 164.7 (CH_{arom}), 119.4, 121.2, 124.7, 136.6, 142.8, 159.9 (C_{arom}). HRMS (ESI+) calcd for C₁₇H₂₁N₆ (M+H)⁺ 309.1822, found 309.1823.

4.1.55 *N*2-(3-(*N,N*-Dimethylamino)propyl)pyrido[3,4-*g*]quinazoline-2,10-diamine (**10g**): 40 h reaction time, obtained as a red oil in quantitative yield. R_f = 0.15 (CH₂Cl₂/NH₃ 7N solution in MeOH 97:3). IR (ATR): 3527-2437, 1607, 1574, 1361 cm⁻¹. ¹H NMR (400 MHz, DMSO-*d*₆) δ 1.87 (2H, quint, *J* = 7.2 Hz), 2.29-2.54 (2H, m), 2.39 (6H, s), 3.50-3.57 (2H, m), 6.33 (2H, br s, NH₂), 7.71 (1H, br s, NH), 7.83 (1H, s), 8.00 (1H, d, *J* = 6.4 Hz), 8.22 (1H, d, *J* = 6.4 Hz), 9.23 (1H, s), 9.33 (1H, s); ¹³C NMR (100 MHz, DMSO-*d*₆) δ 43.9 (2CH₃), 21.1, 38.7, 56.1 (CH₂), 113.6, 115.4, 139.5, 154.7, 164.4 (CH_{arom}), 119.1, 121.2, 124.4, 136.2, 142.4, 159.5 (C_{arom}). HRMS (ESI+) calcd for C₁₆H₂₁N₆ (M+H)⁺ 297.1822, found 297.1823.

4.1.56 *N*2-(3-(*N,N*-Diethylamino)propyl)pyrido[3,4-*g*]quinazoline-2,10-diamine (**10h**): 24 h reaction time, obtained as a red oil 86% in yield. R_f = 0.10 (CH₂Cl₂/NH₃ 7N solution in MeOH 96:4). IR (ATR): 3515-2131, 1606, 1574, 1359, 1198 cm⁻¹. ¹H NMR (400 MHz, DMSO-*d*₆): 1.00

(6H, t, $J = 7.2$ Hz), 1.78 (2H, quint, $J = 7.2$ Hz), 2.50-2.57 (6H, m), 3.47-3.57 (2H, m), 6.29 (2H, br s, NH₂), 7.71 (1H, br s, NH), 7.82 (1H, s), 7.99 (1H, d, $J = 6.0$ Hz), 8.21 (1H, d, $J = 6.0$ Hz), 9.22 (1H, s), 9.32 (1H, s); ¹³C NMR (100 MHz, DMSO-*d*₆): 11.7 (2CH₃), 25.9 (CH₂), 46.3 (2CH₂), 50.5 (CH₂), 113.6, 115.3, 139.5, 154.7, 164.3 (CH_{arom}), 119.1, 121.2, 124.4, 136.0, 144.7, 157.4 (C_{arom}). The missing CH₂ was under the solvent signal. HRMS (ESI+) calcd for C₁₈H₂₅N₆ (M+H)⁺ 325.2135, found 325.2138.

4.1.57 *N2-(3-(Morpholin-1-yl)propyl)pyrido[3,4-g]quinazoline-2,10-diamine (10i)*: 4 h reaction time, obtained as a red oil in 51% yield. $R_f = 0.40$ (CH₂Cl₂/MeOH 9:1) IR (ATR): 3622-2164, 1607, 1575, 1362, 1291, 1111 cm⁻¹. ¹H NMR (400 MHz, DMSO-*d*₆) δ 1.81 (2H, quint, $J = 4.4$ Hz), 2.30-2.55 (6H, m), 3.50-3.54 (2H, m), 3.59-3.62 (4H, m), 6.27 (2H, br s, NH₂), 7.63 (1H, br s, NH), 7.83 (1H, s), 7.99 (1H, d, $J = 4.8$ Hz), 8.22 (1H, d, $J = 4.8$ Hz), 9.23 (1H, s), 9.32 (1H, s); ¹³C NMR (100 MHz, DMSO-*d*₆) δ 25.4, 38.5 (CH₂), 53.4 (2CH₂), 56.2 (CH₂), 66.2 (2CH₂), 113.6, 115.4, 139.5, 154.7, 164.3 (CH_{arom}), 119.1, 121.3, 124.4, 134.7, 136.0, 157.4 (C_{arom}). HRMS (ESI+) calcd for C₁₈H₂₃N₆O (M+H)⁺ 339.1928, found 339.1927. HPLC: purity > 96%, $\lambda = 280$ nm, $t_R = 18.1$ min.

4.1.58 *N2-(3-(N-Methylpiperazin-1-yl)propyl)pyrido[3,4-g]quinazoline-2,10-diamine (10j)*: 18 h reaction time, obtained as a red oil in 56% yield. $R_f = 0.10$ (CH₂Cl₂/NH₃ 7N solution in MeOH 96:4). IR (ATR): 3540-2536, 1608, 1577, 1372, 1284, 1152 cm⁻¹. ¹H NMR (400 MHz, DMSO-*d*₆) δ 1.79 (2H, quint, $J = 5.6$ Hz), 2.16 (3H, s), 2.30-2.56 (8H, m), 2.50-2.53 (2H, m), 3.47-3.54 (2H, m), 6.26 (2H, br s, NH₂), 7.65 (1H, br s, NH), 7.82 (1H, s), 7.98 (1H, d, $J = 5.2$ Hz), 8.21 (1H, d, $J = 5.2$ Hz), 9.22 (1H, s), 9.31 (1H, s); ¹³C NMR (100 MHz, DMSO-*d*₆) δ 45.8 (CH₃), 25.7 (CH₂), 52.7 (2CH₂), 54.8 (2CH₂), 55.9 (CH₂), 113.6, 115.4, 139.5, 154.7, 164.3 (CH_{arom}), 119.1, 121.3, 124.4, 134.7, 136.0, 157.4 (C_{arom}). The missing CH₂ was under the solvent signal. HRMS (ESI+) calcd for C₁₉H₂₆N₇ (M+H)⁺ 352.2244, found 352.2247. HPLC: purity > 96%, $\lambda = 280$ nm, $t_R = 17.9$ min.

4.1.59 *N2-(3-(Piperidin-1-yl)propyl)pyrido[3,4-g]quinazoline-2,10-diamine (10k)*: 40 h reaction time, obtained as a red oil in 18% yield. $R_f = 0.20$ (CH₂Cl₂/NH₃ 7N solution in MeOH 97:3). IR (ATR): 3478-2358, 1607, 1574, 1350 cm⁻¹. ¹H NMR (400 MHz, DMSO-*d*₆): 1.33-1.42 (2H, m), 1.45-1.56 (4H, m), 1.79 (2H, quint, $J = 6.8$ Hz), 2.25-2.43 (6H, m), 3.44-3.57 (2H, m), 6.26 (2H, br s, NH₂), 7.68 (1H, br s, NH), 7.82 (1H, s), 7.98 (1H, d, $J = 6.4$ Hz), 8.21 (1H, d, $J = 6.4$ Hz), 9.22 (1H, s), 9.31 (1H, s); ¹³C NMR (100 MHz, DMSO-*d*₆): 24.0 (CH₂), 25.4 (2CH₂), 42.5 (CH₂), 54.0 (2CH₂), 56.5 (CH₂), 113.6, 115.3, 139.5, 154.7, 165.1 (CH_{arom}), 119.1, 121.6, 124.4, 136.0, 141.7,

160.5 (C_{arom}). The missing CH_2 was under the solvent signal. HRMS (ESI+) calcd for $C_{19}H_{25}N_6$ ($M+H$)⁺ 337.2135, found 337.2136.

4.1.60 *N2-(3-(Pyrrolidin-1-yl)propyl)pyrido[3,4-g]quinazoline-2,10-diamine (10l)*: 18 h reaction time, obtained as a red oil in 63% yield. $R_f = 0.15$ (CH_2Cl_2/NH_3 7N solution in MeOH 97:3). IR (ATR): 3482-2288, 1606, 1574, 1361 cm^{-1} . 1H NMR (400 MHz, DMSO- d_6) δ 1.68-1.76 (4H, m), 1.84 (2H, quint, $J = 7.2$ Hz), 2.42-2.65 (6H, m), 3.48-3.56 (2H, m), 6.28 (2H, br s, NH_2), 7.66 (1H, br s, NH), 7.82 (1H, s), 7.99 (1H, d, $J = 5.8$ Hz), 8.21 (1H, d, $J = 6.0$ Hz), 9.22 (1H, s), 9.31 (1H, s); ^{13}C NMR (100 MHz, DMSO- d_6) δ 22.1 (CH_2), 22.9 (2 CH_2), 29.0, 31.3 (CH_2), 53.5 (2 CH_2), 113.6, 115.4, 139.5, 154.7, 164.4 (CH_{arom}), 119.1, 121.3, 124.4, 136.1, 142.3, 160.2 (C_{arom}). HRMS (ESI+) calcd for $C_{18}H_{23}N_6$ ($M+H$)⁺ 323.1979, found 323.1983.

4.1.61 *N2-Methylpyrido[3,4-g]quinazoline-2,10-diamine (10m)*: due to poor solubility in CH_2Cl_2 , compound **9m** was dissolved in $CH_2Cl_2/MeOH$ 8:2 before reaction for 24 h. Compound **10m** was obtained as a red powder in 58% yield. Mp: degradation. $R_f = 0.20$ ($CH_2Cl_2/MeOH$ 9:1). IR (ATR): 3506-2408, 1579, 1375 cm^{-1} . 1H NMR (400 MHz, DMSO- d_6) δ 3.00 (3H, d, $J = 5.2$ Hz), 6.33 (2H, br s, NH_2), 7.83 (1H, s), 8.00 (1H, d, $J = 6.4$ Hz), 8.15 (1H, br s, NH), 8.22 (1H, d, $J = 6.4$ Hz), 9.23 (1H, s), 9.31 (1H, s); ^{13}C NMR (100 MHz, DMSO- d_6) δ 28.0 (CH_3), 113.5, 115.4, 139.5, 154.7, 164.6 (CH_{arom}), 119.4, 121.7, 124.4, 136.2, 142.5, 160.1 (C_{arom}). HRMS (ESI+) calcd for $C_{12}H_{12}N_5$ ($M+H$)⁺ 226.1087, found 226.1089.

4.2 In vitro kinase inhibition assays

4.2.1. Method A (^{33}P radioassay)

Kinase activities were assayed in appropriate buffer for each kinase, with either protein or peptide as substrate in the presence of 15 μM [γ - ^{33}P] ATP (3,000 Ci/mmol; 10 mCi/ml) in a final volume of 30 μl following the assay described in [20]. Controls were performed with appropriate dilutions of dimethylsulfoxide. Full-length kinases are used unless specified. Peptide substrates were obtained from ProteoGenix (Schiltigheim, France).

HsCDK5/p25 (human, recombinant, expressed in bacteria) was assayed on 0.8 $\mu g/\mu l$ of histone H1 as substrate. SscCK1 δ/ϵ (*Sus scrofa domesticus*, casein kinase 1 δ/ϵ , affinity purified from porcine brain) was assayed on 0.022 $\mu g/\mu l$ of the following peptide: RRKHAAGSpAYSITA as specific substrate. HsCDK5/p25 and SscCK1 δ/ϵ were tested in the following buffer: 60 mM β -

glycerophosphate, 30 mM p-nitrophenyl-phosphate, 25 mM MOPS (pH 7), 5 mM EGTA, 15 mM MgCl₂, 1 mM DTT, 0.1 mM sodium orthovanadate.

*Ssc*GSK-3 α/β (*Sus scrofa domesticus*, glycogen synthase kinase-3, affinity purified from porcine brain) was assayed on 0.01 $\mu\text{g}/\mu\text{l}$ of GS-1 peptide, a GSK-3-selective substrate (YRRAAVPPSPSLSRHSSPHQSpEDEEE, “Sp” stands for phosphorylated serine). *Rn*DYRK1A-kd (*Rattus norvegicus*, kinase domain aa 1 to 499, expressed in bacteria, DNA vector kindly provided by Dr. W. Becker, Aachen, Germany) was assayed on 0.033 $\mu\text{g}/\mu\text{l}$ of the following peptide: KKISGRLSPIMTEQ as substrate. *Mm*CLK1 (from *Mus musculus*, recombinant, expressed in bacteria) was assayed on 0.027 $\mu\text{g}/\mu\text{l}$ of the following peptide: GRSRSRSRSRSR as substrate. *Ssc*GSK-3 α/β , *Rn*DYRK1A and *Mm*CLK1 were tested in the following buffer: 10 mM MgCl₂, 1 mM EGTA, 1 mM DTT, 25 mM Tris-HCl pH 7.5, 50 $\mu\text{g}/\text{ml}$ heparin, 0.15 mg/ml of BSA, 0.23 mg/ml of DTT.

4.2.2. Method B (ADP-glo)

Kinase assays were carried out following ADP-Glo protocol (Promega). Briefly, reactions were carried out in a final volume of 5 μl , at 10 μM ATP, for 30 min at 30 °C. The luminescent signal emitted was measured using an Envision luminometer (PerkinElmer, Waltham, MA) and expressed in Relative Light Unit (RLU).

4.3 In vitro cellular antiproliferative assays

HCT116 cells were cultured in McCoy's 5a medium, SH-SY5Y, MDA-MB231 and U-2 OS cells were cultured in Dulbecco's modified Eagle's medium (DMEM), hTERT RPE1 were cultured in DMEM:F12 medium. All media were supplemented with 10% fetal calf serum, 2 mM L-glutamine, 50 IU penicillin and streptomycin. Cell viability was assayed using CellTiter96 AQueous from PROMEGA according to manufacturer's instructions.

4.4 Protein crystallography

Recombinant CLK1 was expressed and purified as described previously [21]. Two different crystal forms of the apo protein were obtained at 4 °C using the sitting drop vapor diffusion technique by mixing equal volumes of protein solution (7-8 mg/ml protein in 30 mM Hepes, pH 7.5, 300 mM NaCl, 50 mM arginine/glutamine mix 1:1, 0.5 mM TCEP, and 1% v/v glycerol) and the appropriate reservoir solution. Crystal form A grew with a reservoir solution of 25% (w/v) PEG 6000, and 0.1 M bicine, pH 9.0; and crystal form B with a reservoir solution of 29% (v/v) 1,2 propanediol, 0.08 M

Na/K phosphate. Crystal form A was soaked overnight in reservoir solution supplemented with 5 mM **10i** and 25% ethylene glycol, and crystal form B was soaked for 72 h in reservoir solution complemented with 1 mM **9m** and 20% ethylene glycol. Crystals were then flash frozen in liquid nitrogen, and diffraction data were collected at 100 K at BESSY II, beamline 14.2. The datasets were integrated using MOSFLM [22] and scaled with SCALA [23], which are implemented in the CCP4 package [24]. The structures of the two complexes were solved by molecular replacement using PHASER [25] with PDB entry 5JIV as a search model. The structures were then refined using iterative cycles of manual model building in COOT [26] and refinement in REFMAC [27] (CLK1-**10i** complex) or PHENIX [28] (CLK1-**9m** complex). Ligand dictionary files for refinement were generated using the Grade Web Server (<http://grade.globalphasing.org>). Data collection and refinement statistics are summarized in Table 3. Structural figures were prepared using PyMOL (www.pymol.org).

Table 3. X-ray data collection and refinement statistics of CLK1-inhibitor structures

Compound	10i	9m
<i>Data Collection</i>		
Space Group	<i>I</i> 2	<i>P</i> 2 ₁
<i>a</i> , <i>b</i> , <i>c</i> (Å)	72.8, 64.3, 86.3	56.8, 117.6, 91.9
α , β , γ (°)	90.0, 110.0, 90.0	90.0, 99.0, 90.0
Molecules/AU	1	3
Resolution (Å) ^a	64.3 -2.29 (2.37-2.29)	47.1 -3.0 (3.18-3.0)
Unique reflections	16,639	23,961
Completeness (%) ^a	99.0 (97.0)	100 (100)
Multiplicity ^a	4.8 (4.8)	3.5 (3.3)
<i>R</i> _{merge} (%) ^a	8.2 (34.6)	16.2 (61.2)
Mean <i>I</i> / σ (<i>I</i>) ^a	9.1 (3.7)	5.1 (1.6)
<i>Refinement</i>		
<i>R</i> _{work} , (%) ^b	18.8	19.8
<i>R</i> _{free} , (%) ^b	25.9	24.4
No. of atoms		
Protein ^c	2733	7972
Water	133	8
Ligands	50	57
RMSD bonds (Å)	0.014	0.005
RMSD angles (°)	1.8	0.6
Mean <i>B</i> (Å ²)	35.1	33.4
Ramachandran favored (%)	94.9	94.7
Ramachandran outliers (%)	0.3	0.5
PDB entry	6Q8K	6Q8P

^aValues in parentheses are for the highest resolution shell.

^b R_{work} and $R_{\text{free}} = \frac{\sum ||F_{\text{obs}}| - |F_{\text{calc}}||}{\sum |F_{\text{obs}}|}$, where R_{free} was calculated with 5 % of the reflections chosen at random and not used in the refinement.

^cNumber includes alternative conformations.

^dRamachandran statistics were calculated using MolProbity [29].

Acknowledgements

The authors thank Aurélie Job for HPLC analysis. The Auvergne Region (Jeune Chercheur Program) is acknowledged for funding of W. Z., F. A., F. G. and P. M. as well as the French Ministry of Higher Education and Research for Y. J. E. PhD fellowship. H. T. is grateful to the Carthage University (Tunisia) for a doctoral mobility fellowship. KISSf facility is supported by Biogèneouest/Région Bretagne, Cancéropôle Grand Ouest and GIS IBiSA. A.C.J. is funded by German Research Foundation (DFG) grant JO 1473/1-1. We are grateful for support by the SGC, a registered charity (number 1097737) that receives funds from AbbVie, Bayer Pharma AG, Boehringer Ingelheim, Canada Foundation for Innovation, Eshelman Institute for Innovation, Genome Canada through Ontario Genomics Institute, Innovative Medicines Initiative (EU/EFPIA) (ULTRA-DD grant no. 115766), Janssen, Merck & Co., Novartis Pharma AG, Ontario Ministry of Economic Development and Innovation, Pfizer, São Paulo Research Foundation-FAPESP, Takeda, and the Wellcome Trust. We also thank the staff at BESSY II beamline 14.2 for their assistance during data collection.

Accession codes

The atomic coordinates and structure factors of the CLK1-pyrido[3,4-g]quinazoline complexes have been deposited in the Protein Data Bank (PDB), www.pdb.org. Accession codes: 6Q8K (CLK1-**10i** complex) and 6Q8P (CLK1-**9m** complex).

References

- [1] Müller, S.; Chaikuad, A.; Gray, N. S.; Knapp S. The ins and outs of selective kinase inhibitor development. *Nat. Chem. Biol.* **2015**, *11*, 818-821.
- [2] Wu, P.; Nielsen, T. E.; Clausen, H. Small-molecule kinase inhibitors: an analysis of FDA-approved drugs. *Drug Discov. Today* **2016**, *21*, 5-10.
- [3] Esvan, Y. J.; Zeinyeh, W.; Boibessot, T.; Nauton, L.; Théry, V.; Knapp, S.; Chaikuad, A.; Loaëc, N.; Meijer, L.; Anizon, F.; Giraud, F.; Moreau, P. Discovery of pyrido[3,4-g]quinazoline derivatives as CMCG family protein kinase inhibitors: design, synthesis, inhibitory potency and X-ray co-crystal structure. *Eur. J. Med. Chem.* **2016**, *118*, 170-177.
- [4] Abbassi, R.; Johns T. G.; Kassiou, M.; Munoz, L. DYRK1A in neurodegeneration and cancer: molecular basis and clinical implications. *Pharmacol. Ther.* **2015**, *151*, 87-98.

- [5] Schmitt, C.; Miralinaghi, P.; Mariano, M.; Hartmann, R. W.; Engel, M. Hydroxybenzothiophene ketones are efficient pre-mRNA splicing modulators due to dual inhibition of Dyrk1A and Clk1/4. *ACS Med. Chem. Lett.* **2014**, *5*, 963-967.
- [6] Nguyen, T. L.; Fruit, C.; Héroult, Y.; Meijer, L.; Besson, T. Dual-specificity tyrosine phosphorylation-regulated kinase 1A (DYRK1A) inhibitors: a survey of recent patent literature. *Expert Opin. Ther. Pat.* **2017**, *27*, 1183-1199.
- [7] Stotani, S.; Giordanetto, F.; Medda, F. DYRK1A inhibition as potential treatment for Alzheimer's disease. *Future Med. Chem.* **2016**, *8*, 681-696.
- [8] Jain, P.; Karthikeyan, C.; Moorthy, N. S. H; N.; Waiker, D. K.; Jain, A. K.; Trivedi, P. Human CDC2-like kinase 1 (CLK1): a novel target for Alzheimer's disease. *Curr. Drug Targets* **2014**, *15*, 539-550.
- [9] Jarhad, D. B.; Mashelkar, K. K.; Kim, H.-R.; Noh, M.; Jeong, L. S. Dual-specificity tyrosine phosphorylation-regulated kinase 1A (DYRK1A) inhibitors as potential therapeutics. *J. Med. Chem.* **2018**, *61*, 9791-9810.
- [10] Zeinyeh, W.; Esvan, Y. J.; Nauton, L.; Loaëc, N.; Meijer, L.; Théry, V.; Anizon, F.; Giraud, F.; Moreau, P. Synthesis and preliminary in vitro kinase inhibition evaluation of new diversely substituted pyrido[3,4-g]quinazoline derivatives. *Bioorg. Med. Chem. Lett.* **2016**, *26*, 4327-4329.
- [11] Yu, X.-M.; Ramiandrasoa, F.; Guetzoyan, L.; Pradines, B.; Quintino, E.; Gadelle, D; Forterre, P.; Cresteil, T.; Mahy, J.-P.; Pethe, S. Synthesis and biological evaluation of acridine derivatives as antimalarial agents. *ChemMedChem* **2012**, *7*, 587-605.
- [12] Jo, M. N.; Seo, H. J.; Kim, Y.; Seo, S. H.; Rhim, H., Cho, Y. S.; Cha, J. H.; Koh, H. Y.; Choo, H.; Pae, A. N. Novel T-type calcium channel blockers: dioxoquinazoline carboxamide derivatives. *Bioorg. Med. Chem.* **2007**, *15*, 365-373.
- [13] Gros, W.; Nemitz, R.; Kroos, A. Phthalimides as bleach activators. **2011**, WO 2011079974.
- [14] Dickerson, S. H.; Tavares, F. X.; Zhou, H. Pyridazine compounds as GSK-3 inhibitors. **2004**, WO2004035588.
- [15] Zhang, L.; Shan, Y.; Li, C.; Sun, Y.; Su, P.; Wang, J.; Li, L.; Pan, X.; Zhang, J. Discovery of novel anti-angiogenesis agents. Part 6: multi-targeted RTK inhibitors. *Eur. J. Med. Chem.* **2017**, *127*, 275-285.
- [16] Ignasik, M.; Bajda, M.; Guzior, N.; Prinz, M.; Holzgrabe, U.; Malawska, B. Design, synthesis and evaluation of novel 2-(aminoalkyl)-isoindoline-1,3-dione derivatives as dual-binding site acetylcholinesterase inhibitors. *Arch. Pharm. Chem. Life Sci.* **2012**, *345*, 509-516.

- [17] Lavrado, J.; Cabal, G. G.; Prudêncio, M.; Mota, M. M.; Gut, J.; Rosenthal, P. J.; Diaz, C.; Guedes, R. C.; dos Santos, D. J. V. A.; Bichenkova, E.; Douglas, K. T.; Moreira, R.; Paulo, A. Incorporation of basic side chains into cryptolepine scaffold: structure-antimalarial activity relationships and mechanistic studies. *J. Med. Chem.* **2011**, *54*, 734-750.
- [18] Cheng, X.; Rasqué, P.; Vatter, S.; Merz, K.-H.; Eisenbrand G. Synthesis and cytotoxicity of novel indirubin-5-carboxamides. *Bioorg. Med. Chem.* **2010**, *18*, 4509-4515.
- [19] Tapia, I.; Alonso-Cires, L.; López-Tudanca, P. L.; Mosquera, R.; Labeaga, L.; Innerarity, A.; Orjales, A. 2,3-Dihydro-2-oxo-1*H*-benzimidazoles-1-carboxamides with selective affinity for the 5-HT₄ receptor: synthesis and structure-affinity and structure-activity relationships of a new series of partial agonist and antagonist derivatives. *J. Med. Chem.* **1999**, *42*, 2870-2880.
- [20] Bach, S.; Knockaert, M.; Reinhardt, J.; Lozach, O.; Schmitt, S.; Baratte, B.; Koken, M.; Coburn, S. P.; Tang, L.; Jiang, T.; Liang, D.-C.; Galons, H.; Dierick, J. F.; Pinna, L. A.; Meggio, F.; Totzke, F.; Schächtele, C.; Lerman, A. S.; Carnero, A.; Wan, Y.; Gray, N.; Meijer, L. Roscovitine targets, protein kinases and pyridoxal kinase. *J. Biol. Chem.* **2005**, *280*, 31208-31219.
- [21] Bullock, A. N.; Das, S.; Debreczeni, J. E.; Rellos, P.; Fedorov, O.; Niesen, F. H.; Guo, K.; Papagrigoriou, E.; Amos, A. L.; Cho, S.; Turk, B. E.; Ghosh, G.; Knapp, S. Kinase domain insertions define distinct roles of CLK kinases in SR protein phosphorylation. *Structure* **2009**, *17*, 352-362.
- [22] Powell, H. R.; Johnson, O.; Leslie, A. G. W. Autoindexing diffraction images with iMosfilm. *Acta Cryst. D.* **2013**, *69*, 1195-1203.
- [23] Evans, P. Scaling and assessment of data quality. *Acta Cryst. D.* **2006**, *62*, 72-82.
- [24] Winn, M. D.; Ballard, C. C.; Cowtan, K. D.; Dodson, E. J.; Emsley, P.; Evans, P. R.; Keegan, R. M.; Krissinel, E. B.; Leslie, A. G.; McCoy, A.; McNicholas, S. J.; Murshudov, G. N.; Pannu, N. S.; Potterton, E. A.; Powell, H. R.; Read, R. J.; Vagin, A.; Wilson, K. S. Overview of the CCP4 suite and current developments. *Acta Cryst. D.* **2011**, *67*, 235-242.
- [25] McCoy, A. J.; Grosse-Kunstleve, R. W.; Adams, P. D.; Winn, M. D.; Storoni, L. C.; Read, R. J. Phaser crystallographic software. *J. Appl. Crystallogr.* **2007**, *40*, 658-674.
- [26] Emsley, P.; Lohkamp, B.; Scott, W. G.; Cowtan, K. Features and development of Coot. *Acta Cryst. D.* **2010**, *66*, 486-501.
- [27] Murshudov, G. N.; Skubák, P.; Lebedev, A. A.; Pannu, N. S.; Steiner, R. A.; Nicholls, R. A.; Winn, M. D.; Long, F.; Vagin, A. A. REFMAC5 for the refinement of macromolecular crystal structures. *Acta Cryst. D.* **2011**, *67*, 355-367.

[28] Adams, P. D.; Afonine, P. V.; Bunkoczi, G.; Chen, V. B.; Davis, I. W.; Echols, N.; Headd, J. J.; Hung, L. W.; Kapral, G. J.; Grosse-Kunstleve, R. W.; McCoy, A. J.; Moriarty, N. W.; Oeffner, R.; Read, R. J.; Richardson, D. C.; Richardson, J. S.; Terwilliger, T. C.; Zwart, P. H. PHENIX: a comprehensive Python-based system for macromolecular structure solution. *Acta Cryst. D*, **2010**, *66*, 213-221.

[29] Chen, V.B.; Arendal III, W. B.; Headd, J. J.; Keedy, D. A.; Immormino, R. M.; Kapral, G. J.; Murray, L. W.; Richardson, J. S.; Richardson, D. C. MolProbity: all-atom structure validation for macromolecular crystallography. *Acta Cryst. D*. **2010**, *66*, 12-21.